KANSAS-NEBRASKA SEISMICITY STUDIES USING THE KANSAS-NEBRASKA MICROEARTHQUAKE NETWORK

by

Don W. Steeples
Greg M. Hildebrand
Brett C. Bennett
Richard D. Miller
Young-Jun Chung
Ralph W. Knapp

Kansas Geological Survey
The University of Kansas
Lawrence, Kansas 66046

October, 1987

Open-file Report No. 87-35

ABSTRACT

The Kansas Geological Survey (KGS) operates a 15-station seismograph network with stations located in northeast Kansas and southeast Nebraska. The network is supported in part by funding from the United States Nuclear Regulatory Commission (NRC). This report discusses operation of the network and summarizes the results of research that allows a better understanding of the seismicity of the region and the link between the seismicity and the tectonic setting of the region.

TABLE OF CONTENTS

LIST OF TABLES

LIST OF FIGURES

INTRODUCTION

Historical Seismicity and Tectonic Setting

At least 30 felt earthquakes with epicenters in Kansas have been documented since 1867 (DuBois and Wilson, 1978). For comparison, historical earthquakes are shown in Figure 1 and microearthquakes from 10 years' recording are shown in Figure 2. The most serious of the historical earthquakes were Modified Mercalli Intensity VII events that occurred in 1867 and 1906 in the vicinity of Manhattan. Although the geologic structure or structures responsible for these two earthquakes have not been positively identified, the following paragraphs outline the tectonic setting and provide some insight to the probable geologic structure or structures involved.

The proximity of several MM Intensity VII/VIII earthquake epicenters in Kansas, Nebraska, and Oklahoma to the Nemaha Ridge (a buried Precambrian granitic uplift) or the Humboldt Fault (the eastern boundary of the Nemaha Ridge, Figure 3) led early investigators (Lugn, 1935; Lee, 1954) to ascribe the source of seismic activity to movement on these structures. This view is also reflected in the Seismic Risk Map of the United States (Algermissen, 1969) which shows a zone two (moderate damage expected) designation in the vicinity of the Nemaha Ridge.

Docekal (1970) analyzed the isoseismal patterns of Intensity VII/VIII historical earthquakes in the midcontinent and related them to basement configuration, structure, and lithology. From this, he delineated the Midcontinent Seismic Trend, with earthquake occurrence in central Texas; central Oklahoma; northeast Kansas; southeast Nebraska; southeast Minnesota; and the Keweenaw Peninsula, Michigan. He concluded that the stronger earthquakes of the region were genetically related to the Arbuckle, Nemaha/Humboldt, and Keweenawan Mafic Belt (MGA) structures or combinations of them.

More recently, the Midcontinent Geophysical Anomaly (MGA) has been recognized as representing an important structural feature in the Central Stable Region (Synder, 1973). The MGA (Figure 4) extends from the Lake-Superior region southwestward at least to central Kansas and into Oklahoma (King and Zietz, 1971; Chase and Gilmer, 1973).

Yarger (1981) has shown without doubt that the MGA extends southward beyond the Kansas-Oklahoma border. Data presented on page 8532 of Guinness et al. (1982) suggest that the MGA extends as far south as near 32.5N, 99.6W, near Abilene, Texas. The MGA is the largest positive gravity anomaly in North America with a length of more than 1,000 km, a width of 50 to 100 km, and a maximum peak-to-peak amplitude of 160 mgal. It marks a thick sequence of mafic igneous rocks emplaced along a zone of major late Precambrian rifting (Ocola and Meyer, 1973). The structure is bounded by faults at the surface in the Lake-Superior region, and similar bounding faults are inferred from geophysical data in the area to the south where the structure is deeply buried below younger sediments (King and Zietz, 1971). An offset of 50 to 60 km to the northwest in the Nebraska section of the MGA (near the Kansas-Nebraska border) is interpreted by Chase and Gilmer (1973) as a transform fault of the Precambrian rifting. F.W. Wilson (oral communication) has noted that epicenters of all Intensity-VII earthquakes in Kansas, Nebraska, Iowa, and Minnesota lie very close to the transform faults hypothesized by Chase and Gilmer (1973).

There are surface structures associated with the MGA in the Manhattan, Kansas, area. The Abilene Anticline (Jewett, 1941) parallels its southeast flank and the Riley County kimberlite intrusives (Brookings, 1970) lie along the same structural trend. Emplacement of the kimberlites has been associated with right lateral strike-slip movement on a buried fault at the east flank of the Abilene Anticline (Chelikowsky, 1972). The direction of movement is inferred from rotation of rock joints in the area of the possible fault. The relation of the kimberlites to this strike-slip hypothesis is in doubt because the long axis of the intrusions is oriented northwest-southeast, perpendicular to the Abilene Anticline (Cook, 1955). This indicates that the direction of least horizontal compressive stress was perpendicular to the Abilene Anticline at the time the kimberlites were emplaced, a condition incompatible with strike slip parallel to the Abilene Anticline. The Elk Creek, Nebraska, carbonatite (Brookins et al., 1975) also lies along the southeast flank of the MGA not far from the Kansas-Nebraska border. It appears from aeromagnetic evidence (Yarger, 1981) all of these ultramafic intrusions are controlled or at least influenced by the faults bounding the MGA.

Recently, deep seismic reflection data have been gathered by the Consortium for Continental Reflection Profiling (COCORP) across the MGA in Kansas. These data ultimately will go far in assisting in regional interpretation of the relationship of the MGA to the Nemaha Ridge (Serpa et al., 1984) and in constructing a geologic cross-section of the MGA itself. Data from the eastern section of the COCORP line show the relatively flat-lying sediments in the Forest City basin and complex structures within the Precambrian basement at depths of 10 to 20 km (Brown et al., 1983). The deep Precambrian structures become more shallow in the vicinity of the MGA and the Nemaha Ridge, suggesting 2 to 3 km of uplift since the mid-Precambrian. The age of the uplift may well be Keweenawan, associated with the rifting.

The COCORP data from the MGA vicinity (Serpa et al., 1984) indicate that the Rice Formation reaches a thickness of as much as 3 to 4 km along the flanks of the MGA. The basalt flows within the MGA itself reach a thickness of about 8 km, also. Preliminary interpretation of these latest COCORP data suggest that he Humboldt Fault zone dips about 20-30 to the east and that the Humboldt may be a reactivation of late Precambrian aged faults associated with the formation of the MGA. Faults with similar dips are present on both sides of the central portion of the MGA.

THE KANSAS-NEBRASKA MICROEARTHQUAKE NETWORK

The proposed siting of nuclear power plants in eastern Kansas, southeastern Nebraska, and northeastern Oklahoma, as well as the proposed location of flood control reservoirs over the trace of the Humboldt Fault zone in Pottawatomie and Chase counties, Kansas, have emphasized the need for a better understanding of seismic activity in Kansas. The Kansas Geological Survey (KGS), a research division of the University of Kansas, receives several calls per year from architects and engineers seeking earthquake design criteria for structures and insurance representatives seeking information to be used in risk and potential damage evaluations in Kansas. We can now provide better guidance to these individuals as a result of the research reported here.

The KGS has had a contract with the U.S. Nuclear Regulatory Commission (NRC) to study earthquakes and seismic risk in Kansas for the last 10 years (1977-1987). Our contract with the NRC is part of a multi-state study that also involves state geological surveys in Minnesota, Oklahoma, Nebraska, and Iowa. The KGS has established a fifteen-station microearthquake network in Nebraska and Kansas (Figure 5) as part of the total program. Since 1982 two other separately funded projects have led to additional knowledge of the seismicity in the study region. Between 1982 and 1984, the U.S. Geological Survey contracted with the Geology Department at the University of Kansas to establish a network of eight stations near McCook, Nebraska to investigate the possibility of induced seismicity in the Sleepy Hollow oil field. From July 1986 until March 1987, the University of Kansas and Lawrence Livermore National Laboratory jointly deployed a thirteen-station, 3-component seismic array in Elk County, Kansas to study the properties of wave propagation in the region of southeast Kansas.

The purpose of the total KGS seismic program is to attempt to relate earthquakes to specific fault zones or tectonic features and to estimate the relative seismicity of various regions by understanding the tectonic features which interact to cause the earthquakes. The station configuration in Figure 5 is designed to provide detection and location capability for microearthquakes down to about local magnitude 1.5 along the previously discussed geologic features in eastern Kansas as established by Sheehan and Steeples (1983) and shown in Figures 6 and 7. Locations for earthquakes in eastern Nebraska are attainable down to about local magnitude 1.7 with the new network. The Sleepy-Hollow network in Nebraska was designed specifically to examine earthquakes in that vicinity down to about local magnitude-1.

Instrumentation

The seismic network data are telemetered to the KGS offices at the University of Kansas in Lawrence, Kansas, on long distance voice-grade telephone lines. Data lines are multiplexed where possible to decrease costs of telemetry. Recording is done with translating ink pen on rotating papercovered drums. In addition, a digital earthquake recording system has been on line since January, 1985; it has recorded 32 local and regional earthquakes (Table 2) as well as over 40 quarry blasts. The network has had an operational efficiency record of 97.8% for the previous four year period (Table 4).

BOREHOLE SEISMOMETER EXPERIMENTS

Each station has been equipped with a borehole seismometer in a cased borehole 15 to 50 meters deep depending on local near-surface geology and environmental noise. Boreholes are useful in eliminating local cultural noise and, to some degree, in improving the signal-to-noise ratio, particularly at frequencies in the 10 Hz range or higher as described in the discussion below.

The depth of 15 to 50 meters was chosen partially for economic reasons and partially for seismological reasons. Drilling is relatively expensive, installation costs go up almost exponentially with increasing casing diameter and depth. Installation costs for our stations including drilling, casing, cement and telephone line installation average slightly less than $800 per station. From a seismological point of view it is desirable to place the seismometer below the surface to avoid cultural noise such as vehicular traffic and trains. However, if the seismometer is a large fraction of a seismic wavelength beneath the surface, some waveforms can be distorted by energy reflected downward from the earth's surface. Since the highest frequencies we are interested in are of the order of 10 to 15 Hz and average, P-wave velocity in the upper 50 meters at our station sites is roughly 3 km/sec, the minimum wavelength of seismic data of interest is about 200 meters. Hence, the boreholes are less then one-fourth wavelength deep for the highest frequency of interest.

It has been our experience that the boreholes are of little use in eliminating train noise which is mostly surface waves peaked in the 2 to 3 Hz part of the spectrum. These wavelengths are in the range of 600 to 1000 meters, several times our borehole depth. The elimination of most of the noise from trains would require boreholes perhaps several hundred meters deep.

Local vehicular traffic and noise caused by such things as domestic livestock, however, are effectively reduced by our shallow boreholes. We have performed some experiments to examine the advantages of the use of our shallow boreholes. Figure 8 shows two similar blasts from a quarry in southeast Kansas about 180 km distant from the edge of our network that were recorded at Belvue (BEK) and Emporia (EMK). Both events at Emporia were recorded with a 10 Hz exploration-type digital-grade geophone at the surface. The first (August) blast was recorded at Belvue at the surface with an identical geophone, the second (September) was recorded with an identical geophone at the bottom of a 51-meter borehole. Using the Emporia records to normalize the Belvue records to the same size event, a 10 dB gain was experienced by moving the geophone to the bottom of the borehole. Six dB was attributed to higher instrumentation gain and 4 dB was attributed to decreased attenuation in the weathered surface layers or to slightly different wave propagation characteristics for the two blasts.

Figure 9 and Figure 10 show the advantages of using boreholes with respect to such cultural noise sources as large animals in the vicinity of the seismograph station. There also appears to be some advantage in the use of a very long vertically-buried pipe with the geophone rigidly connected to the top of the pipe, as the amplitudes generated by the man running are smaller for the geophone connected to the top of the pipe than for the two geophones at the surface. These traces were all recorded simultaneously with a digital exploration seismograph. Note the bottom (borehole) trace on Figure 9 where the amplitude of the waves generated by a man running appears to be zero. Note also that in Figure 10 the bottom (borehole) trace has a visible amplitude when Automatic Gain Control (AGC) is used to blow up amplitudes on that trace only. The fact that only the three-foot impacts of closest approach appear on the trace with AGC suggests that the energy recorded at the bottom of the borehole represents some mode that propagated down the pipe rather than directly through the rocks.

More recently, experiments with borehole seismometers at the Sleepy-Hollow network have shown that cultural noise from traffic about 100 meters from the seismometer can be decreased as much as 24 dB by placing the seismometer in boreholes as shallow as 20 meters deep.

RESULTS FROM TEN YEARS RECORDING

Historical earthquakes can often be linked to specific geologic features by inference from the recording of present-day microearthquakes. The microearthquakes pattern shown in Figure 2 bears a very striking resemblance to that shown by historical earthquakes in Figure 1. This result in conjunction with other geological and geophysical studies of the past few years at the KGS allows us to make useful observations about earthquake activity in Kansas. While Cole (1976) showed a single long Humboldt fault in the basement, more recent geophysical evidence (Steeples, 1982) indicates that a zone of faulting perhaps tens of kilometers wide exists along both sides of the Nemaha Ridge. This conclusion is drawn in part from the scatter in both the historical and microearthquake seismicity and in part from other geological and geophysical evidence. Seismic reflection surveys, including unpublished proprietary data, indicate a myriad of faulting along both sides of the Nemaha Ridge. Gravity and aeromagnetic data are consistent with a multitude of unmapped faults. Drawing on these data and LANDSAT lineaments, Berendsen, (1984) has examined cuttings from hundreds of wells on both sides of the Nemaha and has hypothesized faulting between basement crustal blocks.

At first this might seem to indicate increased earthquake risk in the Nemaha Ridge vicinity. This interpretation, based on large amounts of new data, does not increase the likely maximum length of known faults. Hence, the maximum expected earthquake is not increased by the new data. It is possible, however, for earthquakes up to body-wave magnitude 5 to 5 to occur in the future on faults auxiliary to the Humboldt fault, or on faults associated with he boundaries of the MGA. With this idea in mind, discussion of seismicity in Kansas follows.

The occurrence of microearthquakes along the approximate trace of the Humboldt fault zone implies the possible occurrence in the past and future of larger earthquakes. Previously unknown felt reports from the 1867 so-called"Manhattan earthquake" (Modified Mercalli Intensity VII) suggest that the epicenter may have been east of Manhattan near the known Humboldt fault trace (DuBois and Wilson, 1978) rather than "22 miles northwest of Manhattan"(Merriam, 1956). Several more years of microearthquake data will be required in conjunction with historical earthquake data to estimate the average return period for the 1867-type earthquake.

The series of felt earthquakes in the Manhattan vicinity in 1929 are no longer as enigmatic in regard to their structural source. Isoseismal patterns clearly indicate that the epicenters were 20 to 40 km west of the main trace of the Humboldt fault. As detailed earlier, however, there are other structures in the Manhattan area that may be responsible for some of the historical earthquakes. The pattern of microearthquakes along the Nemaha Ridge is diverse, suggesting that several faults are capable of producing small to moderate earthquakes. At least one microearthquake has occurred in the area south of Junction City, at least 20 km west of the Humboldt fault.

Several epicenters of both historic earthquakes and microearthquakes in northwest Kansas have not yet been discussed in this report. The seismicity pattern of the past ten years coupled with several historical epicenter (Woolard, 1958) suggests that some low to moderate level of tectonic activity is occurring along this whole structure in central and northwest Kansas and in western Nebraska. A long-term trend of such tectonic movement is explicitly suggested by Stanley and Wayne (1972) on the basis of drainage and sedimentation patterns in the area during the Pleistocene Epoch and by present-day stream gradients and kick points on several rivers that cross the structural trend.

The earthquakes located using the Kansas-Nebraska Network, tend to fall into four distinct geologic trends (Appendix A). A large portion of the events lie astride the Nemaha Ridge and indicate low levels of seismicity on faults associated with or bounding the ridge. A trend of events roughly parallel to the ridge, but about 100 km to the west of it is associated with the Midcontinent Geophysical Anomaly (MGA). Intersecting these trends from the northwest is a belt of earthquake activity that during the first five to six years of network operation had only sparse activity; however, recently a marked increase in earthquake activity has been observed. This northwest-southeast trend seems to be related to the faults flanking the Central Kansas Uplift. Lastly, but least understood geologically, is a trend of earthquakes that extends in a northeast-southwest direction across central Nebraska. This trend of earthquakes has no named geologic structure associated with it but there are a pair of faults shown on the USGS/ AAPG Tectonic map that are coincident with the trend. The central-Nebraska trend intersects the Central Kansas Uplift at nearly a right angle. There is a strong concentration of seismicity at that intersection.

The recent increased earthquake activity along the Central Kansas Uplift has been documented on earthquake seismograms and by earthquake-felt reports. The majority of the felt reports from the 7 to 8 events with sufficient size to be felt were from areas within Rooks, Graham, and Ellis counties. The group of events responsible for most of these felt reports can be clearly identified on the microearthquake epicenter map (Figure 2).

A single event recorded with an epicenter near Lakin, Kansas, was of sufficient size (MDUR=3.0) to be felt by people over a relatively small area. The lack of any located epicenters below MDUR=3.0 in the area is not surprising with the lack of sensitivity of the network that far from the primary monitoring area, the Nemaha Ridge (Figure 3).

Perhaps one of the most critical and important observations with respect to seismic activity in western Kansas and central Nebraska is that the two trends intersect at the Sleepy Hollow oil field. Because of that intersection, we believe that the Sleepy Hollow earthquakes (at least some of them) are tectonic in nature rather than induced by water-flood operations in the oil field. It is worth noting that other water-flood operations within oil fields along the Central Kansas Uplift do not cause earthquake activity,further suggesting that the earthquakes at Sleepy Hollow are tectonic.

Recent earthquake analysis has involved both digital data and standard drum-recorded analog data. Refraction-type crust/mantle studies (Miller,1983, Steeples and Miller, in press (Appendix B)) have included both earthquake data from the Kansas-Nebraska network and explosion refraction data. The general seismicity (Evans and Steeples, 1987) and an estimation of the source parameters of earthquakes in the Sleepy Hollow oil field in Red Willow County, Nebraska (Wallace et. al, in review), have been derived from analysis of microearthquake data. The earthquake data sets are continuously updated in order to determine more representative composite interpretations of crust/mantle structures and properties.

CONCLUSIONS

1. The microearthquake pattern established over a ten-year period in the Kansas vicinity bears striking resemblance to the historical pattern established over the past 125 years of recorded history.

2. The vast majority of the microearthquakes in Kansas can be related directly to the Nemaha Ridge/Humboldt Fault zone, the Midcontinent

Geophysical Anomaly and its southward extension into Oklahoma, and the Central Kansas Uplift.

3. A large number of faults exist in the vicinity of these major structures. These faults are likely capable of generating earthquakes in the body wave magnitude range of 5 to 5 1/2.

4. At least some of the earthquakes in the Sleepy Hollow oil field in southwestern Nebraska are likely tectonic because the seismic activity lies at the intersection of the Central Kansas Uplift and an unnamed northeastward trend that extends some 350 km across Nebraska.

5. A comparison of microearthquakes recorded during the first 5 year period (Figure 11) and those recorded during the second five year period (Figure 12), indicate that no new seismic trends have occurred during the latter recording period, although the activity to the west has increased somewhat.

REFERENCES

Algermissen, S.T., 1969, Seismic risk studies in the United States: Proc. of Fourth World Conf. on Earthquake Engr., Santiago, Chile, v. 1, p. 14-27.

Berendsen, P., 1984, Structural development of basement and overlying rocks across the Central North American Rift System, central Kansas: Kansas Geological Survey (in press).

(Brookings, 1970)

Brookins, D.G., Treves, S.B., and Bolivar, S.L. 1975, Elk Creek, Nebraska, carbonatite: Strontium Geochemistry, Earth and Planetary Science Letters, 28, p. 79-82.

Brown, L., et al., 1983 Intracrustal complexity in the United States Midcontinent: Preliminary results from COCORP surveys in northeastern Kansas: Geology, v. 11, p. 25-30.

Chase, C.G., and Gilmer, T.H., 1973, Precambrian plate tectonics: The Midcontinent gravity high: Earth and Planetary Science Letters, 21, p. 70-78.

Chelikowsky, J.R., 1972, Structural geology of the Manhattan, Kansas area: Kansas Geological Survey Bull. 204, pt. 4,.

Cole, V.B., 1976, Configuration of the top of the Precambrian rocks in Kansas: Kansas Geological Survey Map M-7, scale 1:5000,000, 1 sheet.

Cook, K.L., 1955, Magnetic surveys over serpentine masses, Riley County, Kansas: Mining Engineering, v. 7, no. 5, p. 481-488.

Docekal, J., 1970, Earthquakes of the Stable Interior, with emphasis on the Midcontinent, Ph.D. thesis, University of Nebraska.

DuBois, S.M., and Wilson, F.W., 1978, List of earthquake intensities for Kansas, 1867-1977: Kansas Geological Survey, Environmental Geology Series 2.

Evans, D.G., and D.W. Steeples, 1987, Microearthquakes near the Sleepy Hollow Oil Field, southwestern Nebraska: Seismological Society of America Bull., v. 77, p. 132-140.

Guinness, E.A., et al., 1982, Identification of a Precambrian rift through Missouri by digital image processing of geophysical and geologic data: Jour. Geophysical Research, v. 87, no. B10, p. 8532.

Jewett, J.M., 1941, The geology of Riley and Geary counties, Kansas: Kansas Geological Survey Bull. 39.

King, E.R. and Zietz, I., 1971, Aeromagnetic study of the Midcontinent gravity high of central United States: Geol. Soc. Am. Bull., v. 82, p. 2187-2208.

Lee, W.H.K. and Lahr, J.C., 1972, HYPO71: A computer program for determining hypocenter, magnitude, and first-motion pattern of local earthquakes: U.S. Geological Survey Open File Report, 100 p.

Lee, W.H.K., 1954, Earthquakes and Nemaha anticline: Am. Assoc. Petr. Geol. Bull, v. 38, no. 2, p. 338-340.

Lugn, A.L., 1935, The Nebraska earthquake of March 1, 1935: Science, v. 81, no. 2102, p. 338-339.

Merriam, D.F., 1956, History of earthquakes in Kansas: Seismol. Soc. Am. Bull. 46, p. 87-96.

Miller, R.D., 1983, Crustal structure in Kansas from regional earthquake seismograms: M.S. thesis, Department of Physics, University of Kansas, Lawrence, Kansas Geological Survey Open-file Report 83-21.

Ocola, L.C. and Meyer, R.P., 1973, Central North American Rift System 1. Structure of the axial zone from seismic and gravimetric data: Jour. Geophysical Research, 78, p. 5173-5194.

Serpa, L., Setzer, T., Farmer, H., Brown, L., Oliver, J., Kaufman, S., Sharp, J., and Steeples, D.W., 1984, Structure of the southern Keweenawan rift from COCORP surveys across the Midcontinent Geophysical Anomaly in northeastern Kansas: Tectonics, v. 3, p. 367-384.

Sheehan, A.F., and D.W. Steeples, 1983, Sensitivity of Kansas microearthquake network: Earthquake Notes, v. 54, no. 2, p. 13-21.

Snyder, F.G., 1968, Tectonic history of Midcontinental United States: UMR Journal, no. 1, p. 65-77.

Stanley, K.O. and Wayne, W.J., 1972, Epeirogenic and climatic controls of early Pleistocene fluvial sediment dispersal in Nebraska: Geol. Soc. Am.Bull., v. 83, p. 3675-3690.

Steeples, D.W., 1982, Structure of the Salina-Forest City interbasin boundary area from seismic studies: University of Missouri, Rolla, Journal, no. 3, p. 55-81.

Steeples, D.W., and R.D. Miller, 1987, Kansas refraction profiles: Proc. of Symposium on Geophysics in Kansas - a 25-year update, Nov. 1984, Kansas Geological Survey Bull. 226, in press.

Wallace, K.D., D.G. Evans, and D.W. Steeples, Source parameters for microearthquakes near the Sleepy Hollow Oil Field, southwestern Nebraska: Submitted to Seismological Society of America Bull., in review March 1987.

Woolard, G.P., 1958, Areas of tectonic activity as indicated by earthquake epicenters: Am. Geophys. Union Trans., v. 39, p. 1135-1150.

Yarger, H.L., 1981, Aeromagnetic survey of Kansas: EOS (Am. Geophys. Union Trans.), v. 62, no. 17, p. 173-178.

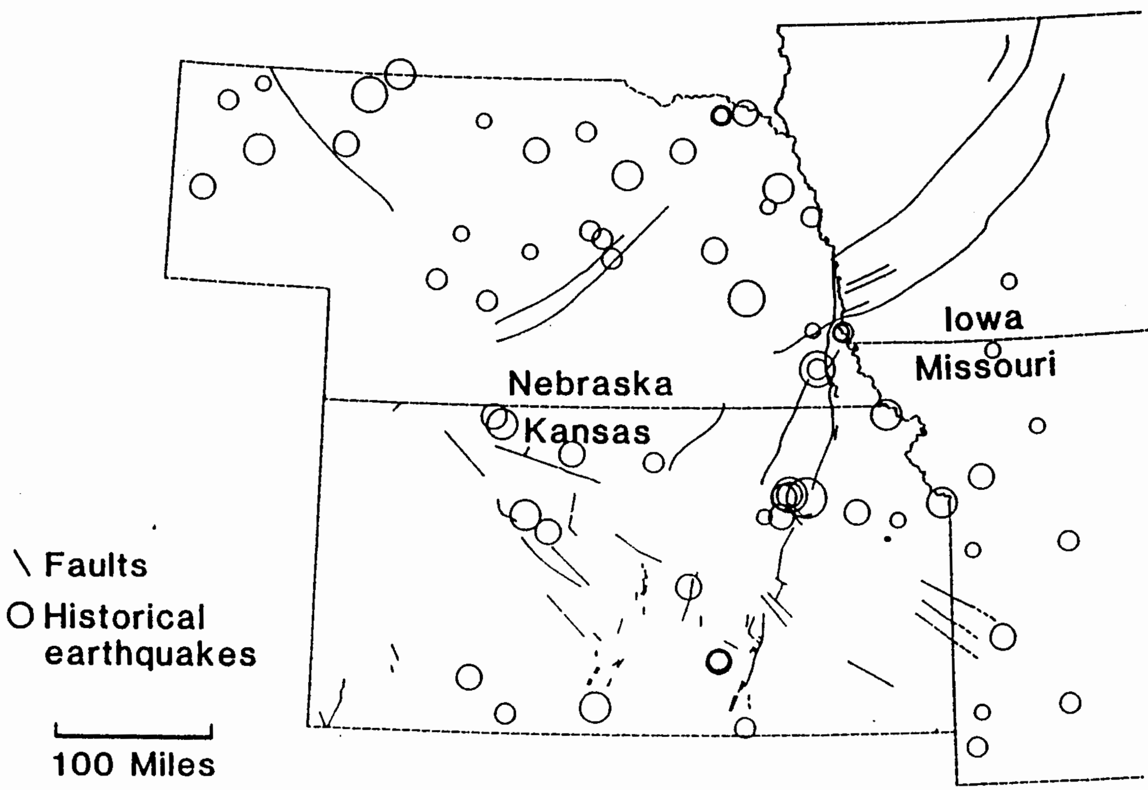

Figure 1. Historical earthquakes are shown by size-coded circles of Modified Mercalli Intensity. Largest events are in the MM VII range. Faults are depicted by lines and are taken from many sources in the literature.

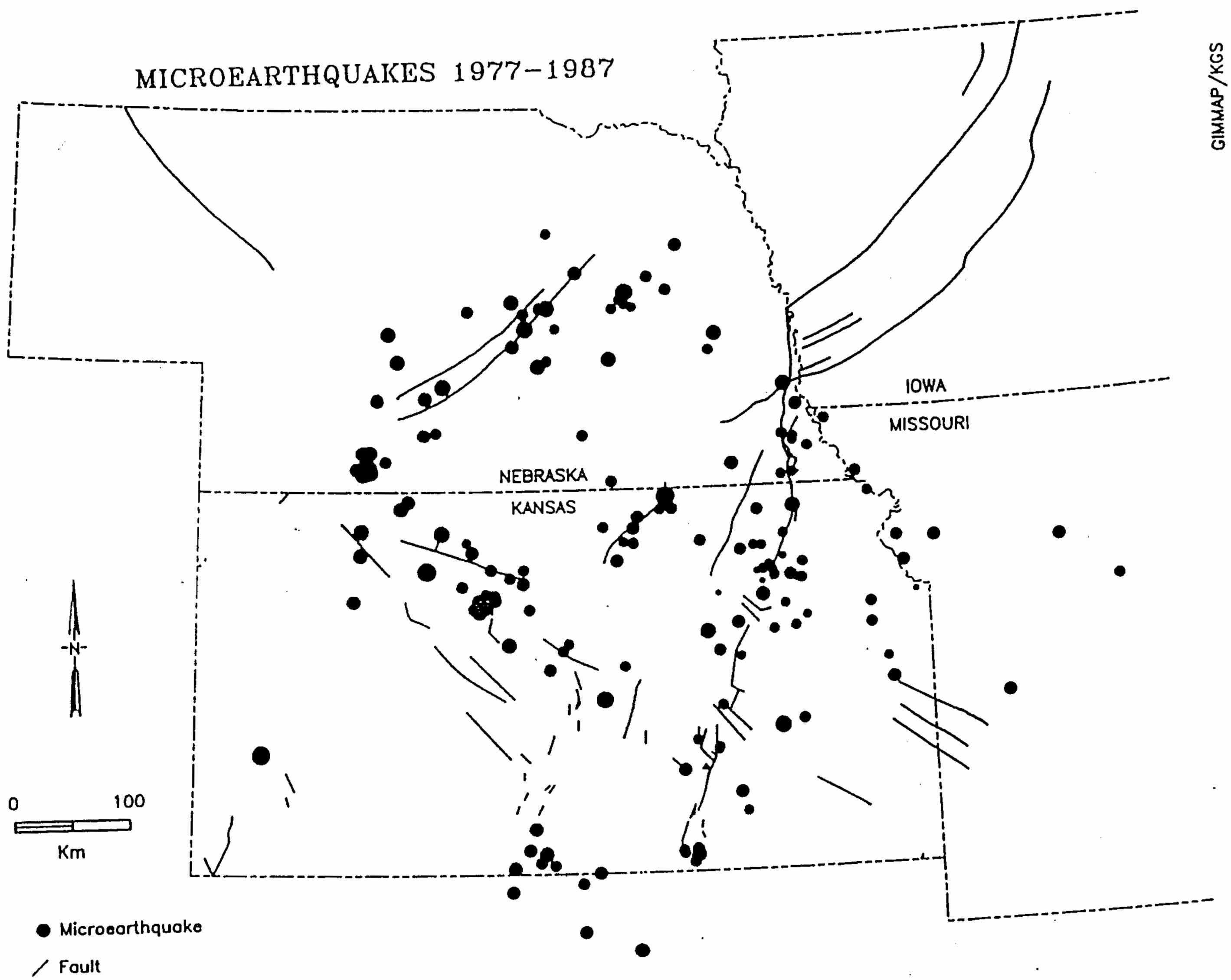

Figure 2. Microearthquakes, recorded by the Kansas Geological Survey between August 1977, and June 1987, are size coded by local magnitude. The largest event has a magnitude 3.3 and the smallest is local magnitude 0.8. Faults plotted are identical to figure 1.

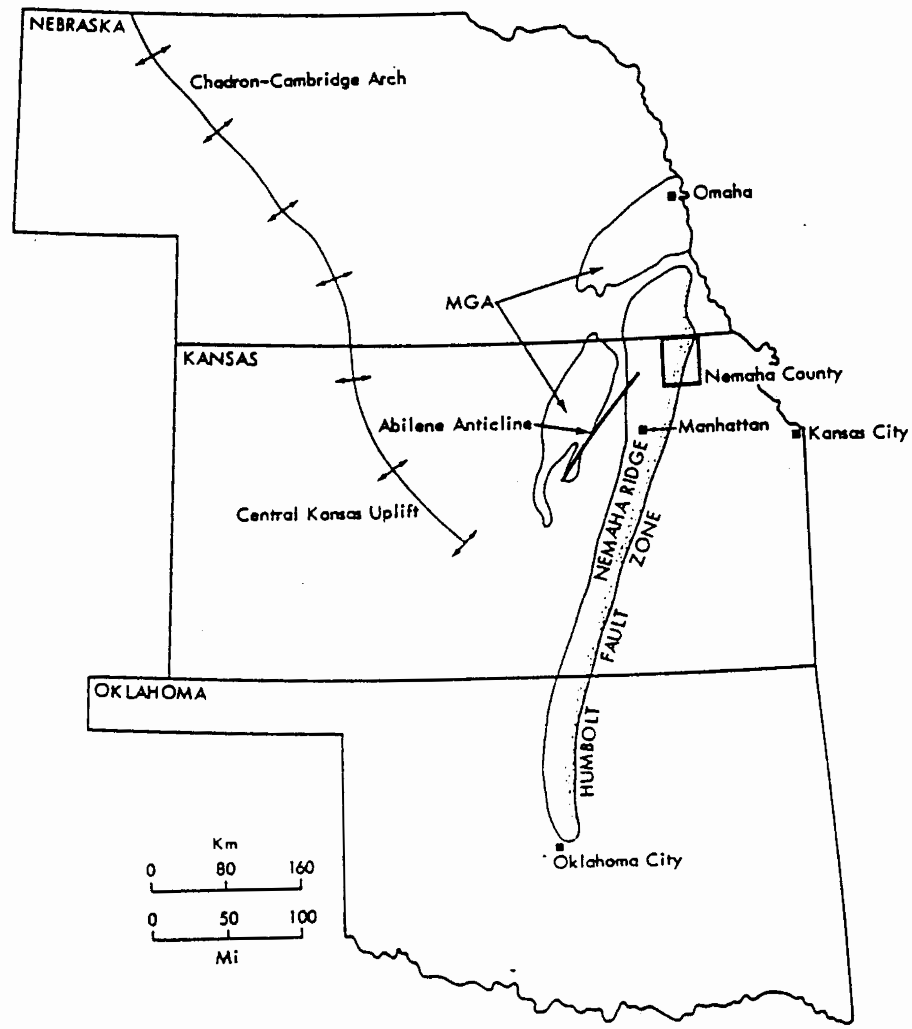

Figure 3. Major regional tectonic features that are apparently related to earthquake activity. Nemaha County is the locality where the Nemaha Ridge was discovered by drilling in the early 1900's.

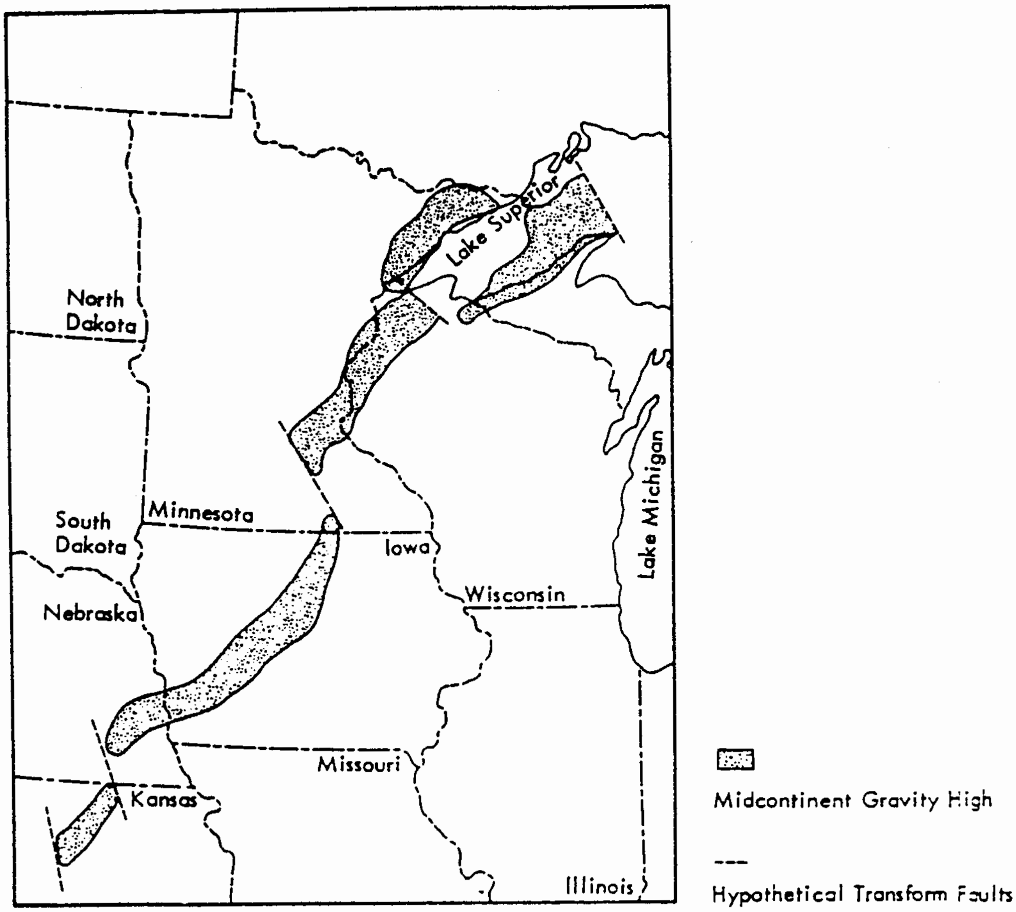

Figure 4. Regional extent of the MGA, modified from Chase and Gilmer (1973).

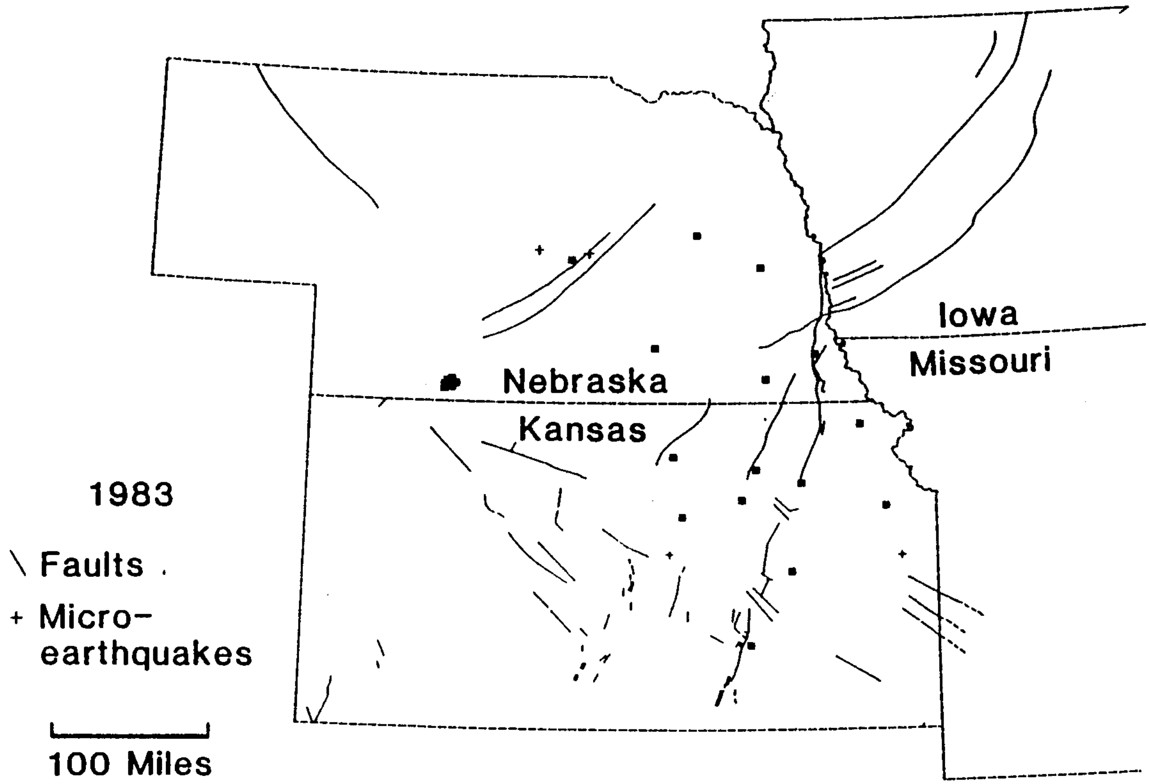

Figure 5 Stations of the Kansas-Nebraska seismograph network after December 1, 1982, are shown by solid squares. The Sleepy Hollow seismograph network is a dense network of eight stations in southwestern Nebraska. The Indianola, Nebraska, station was operated for two years using local on-site recording near the center of that present network.

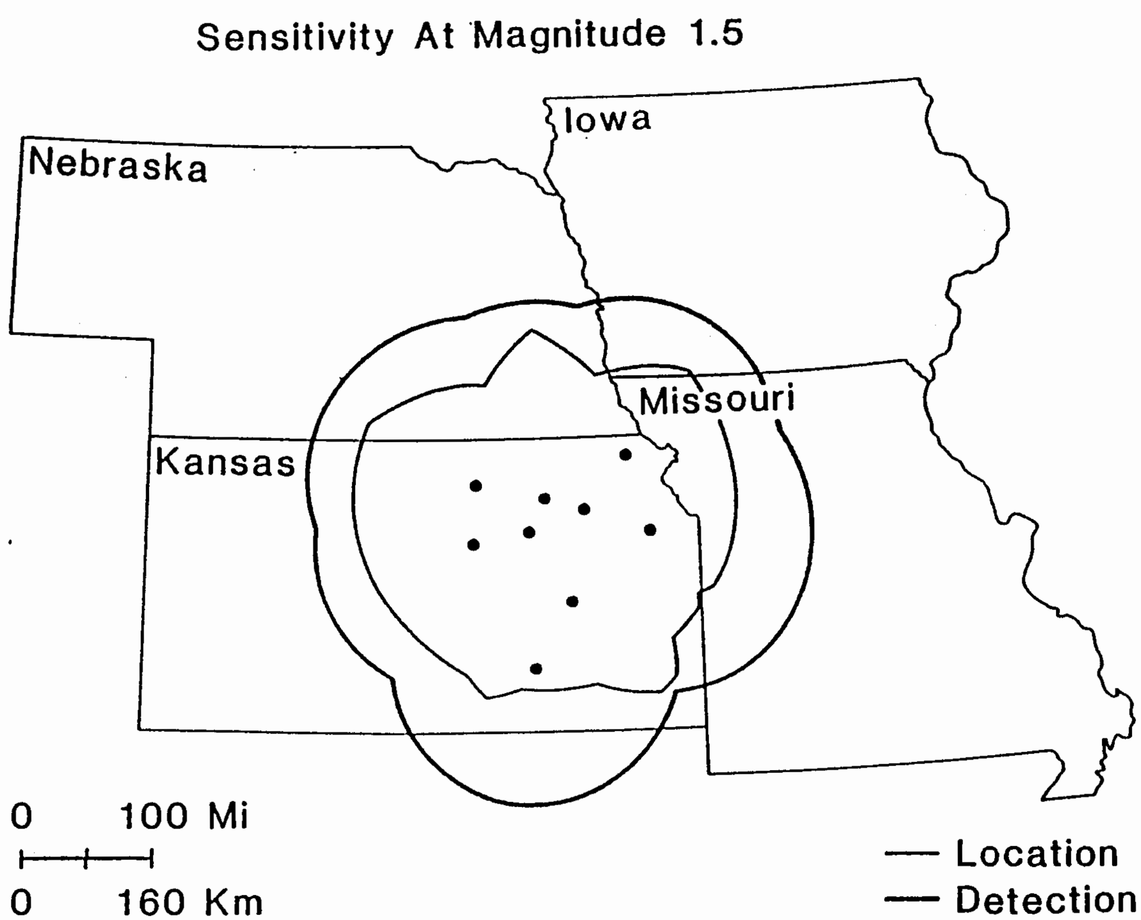

Figure 6. The sensitivity of the network at local magnitude 1.5 is shown. The outer closed curve is detection sensitivity. The inner closed curve is location sensitivity, based upon detection by at least three stations.

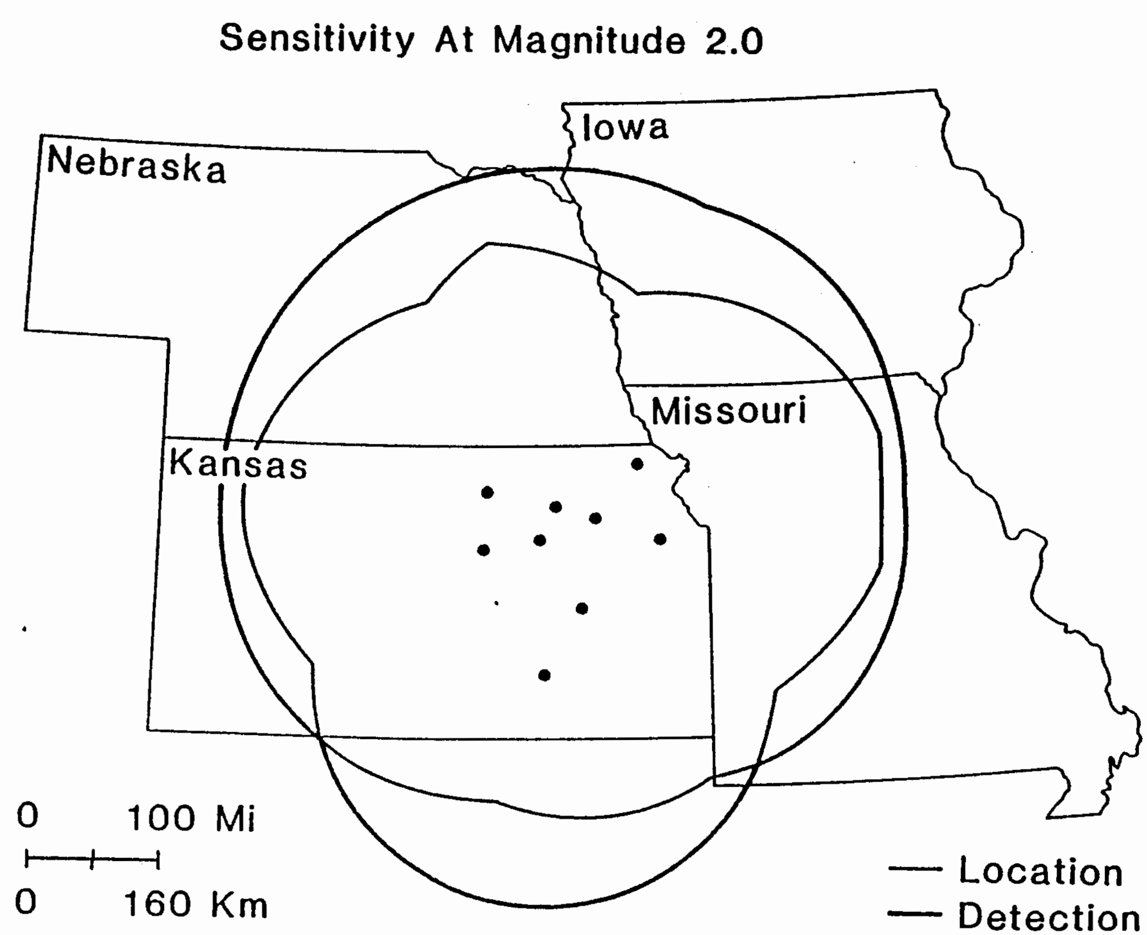

Figure 6a. Sensitivity of the network to earthquakes of local magnitude 2.0. The inner closed curve is for location by detection at three or more stations. The outer closed curve is for detection at only one station.

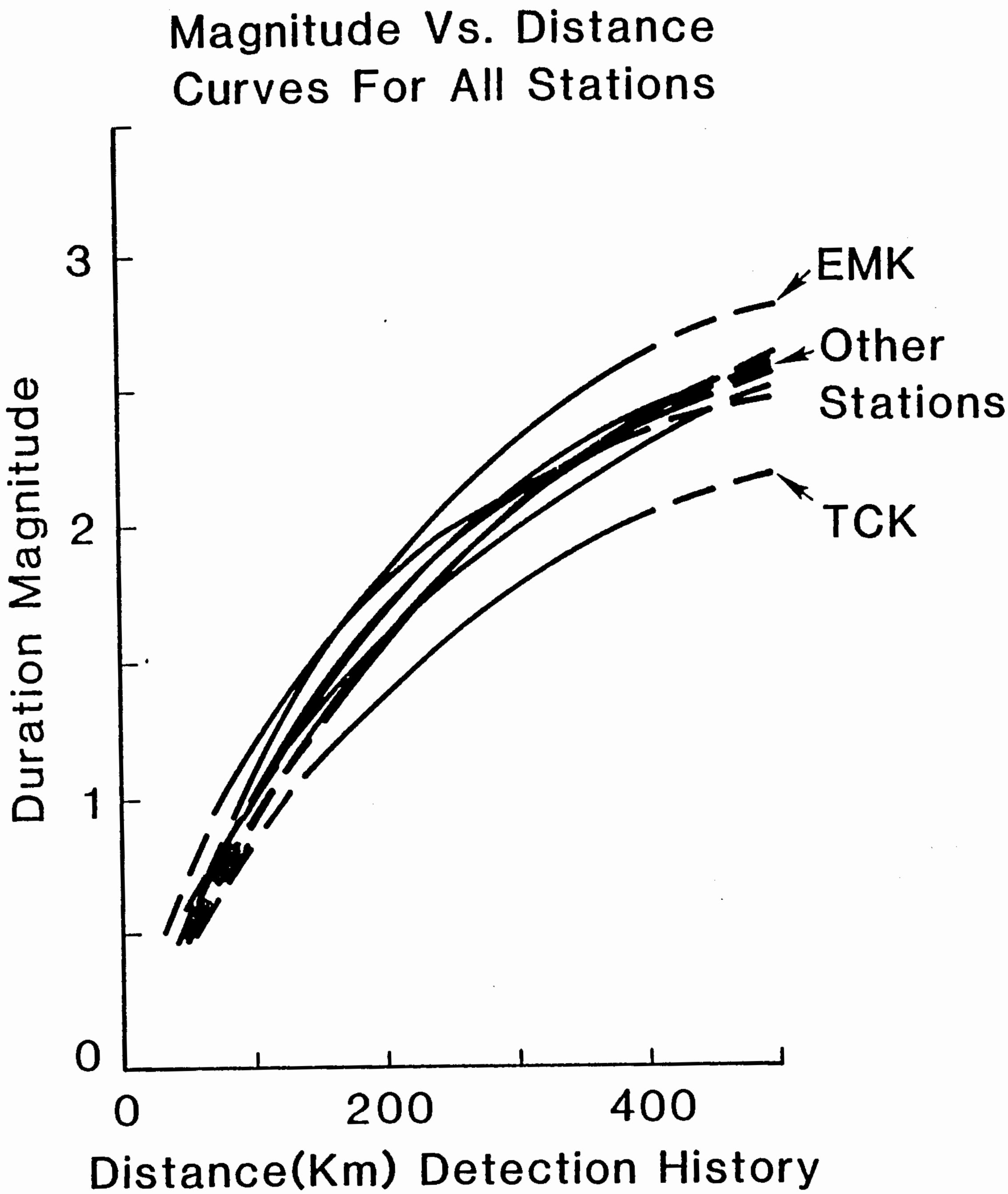

Figure 7. Magnitude versus detection history curves used in preparation of Figure 6.

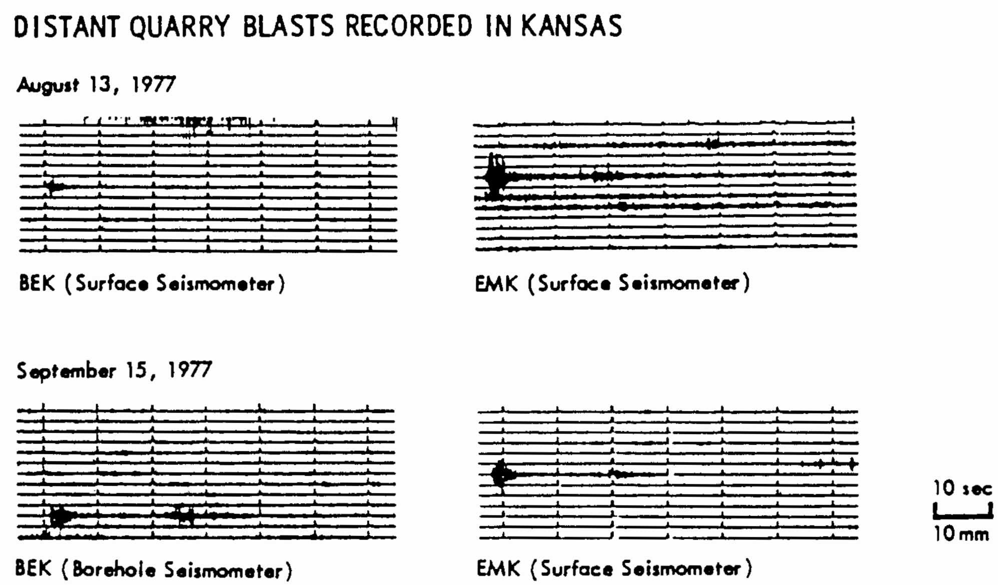

Figure 8. Blasts from 180 km distant quarry recorded on August 13 and September 15, 1977, at BEK and EMK. Note that signal recorded by borehole seismometer is considerably enhanced.

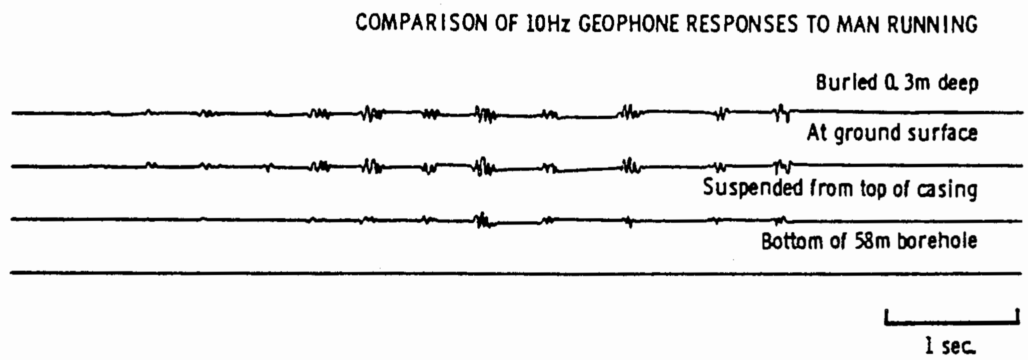

Figure 9. Response of four identical geophones (three at or very near top of borehole) to 100 kg man running from 15 meters from borehole to within two meters of borehole and to 15 meters beyond borehole. Note that using identical plotting and recording parameters, signal at bottom of borehole appears to be missing.

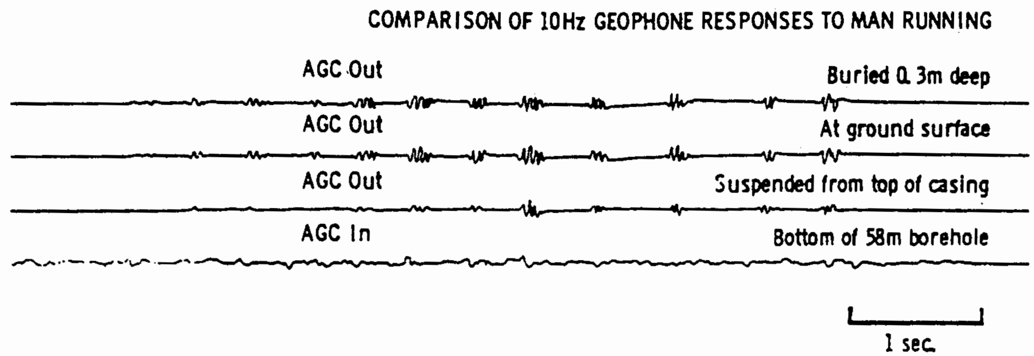

Figure 10. Identical to data in Figure 9, except Automatic Gain Control (AGC) was used to expand amplitudes on trace from borehole geophone. Note that on the three foot impacts nearest the borehole (near the center of the record) some signal propagated to the bottom of the borehole.

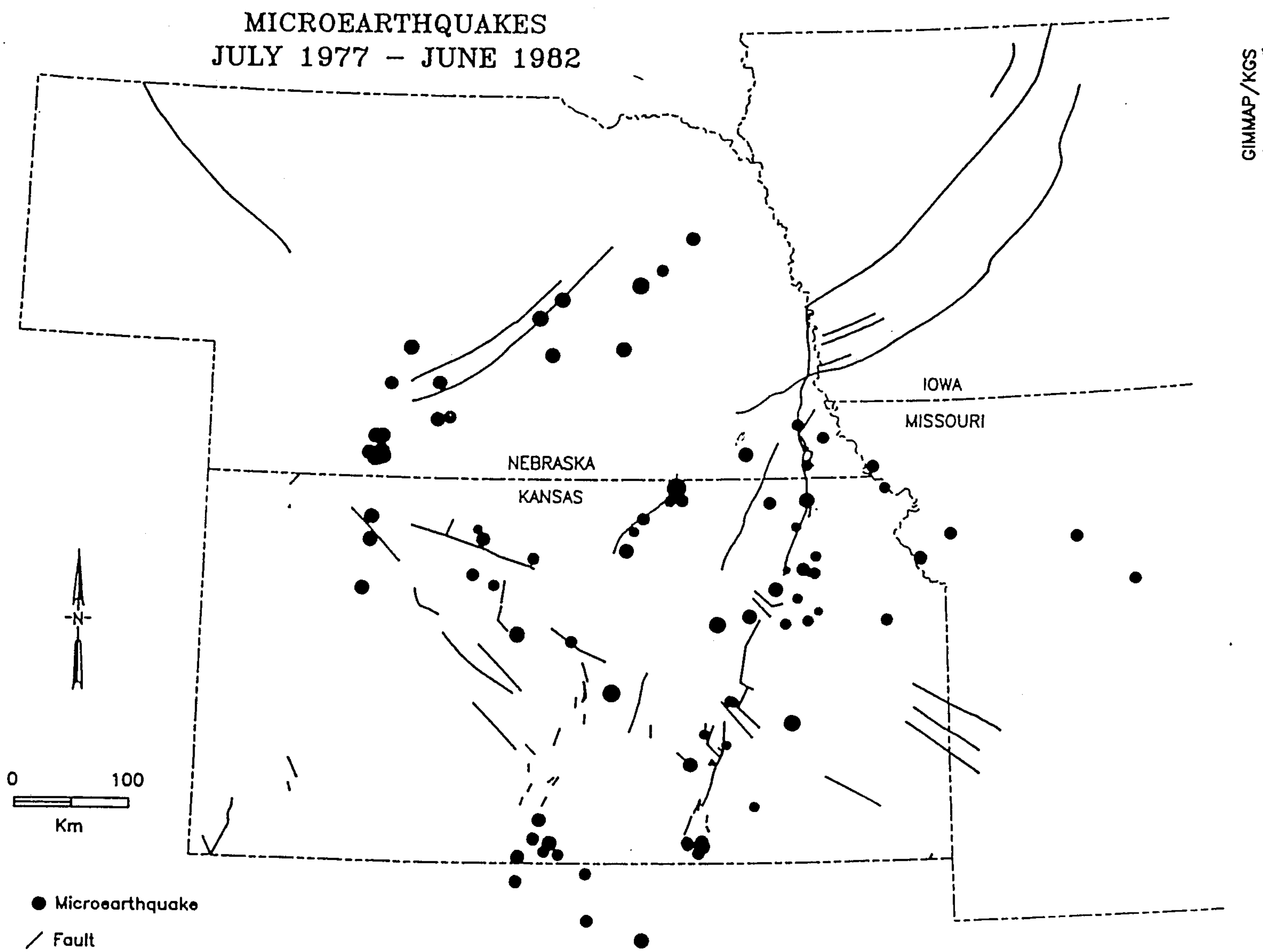
MICROEARTHQUAKES
JULY 1977 - JUNE 1982
GIMMAP/KGS
IOWA
MISSOURI
NEBRASKA
KANSAS
N
0
100
Km
Microearthquake
Fault

Figure 11.

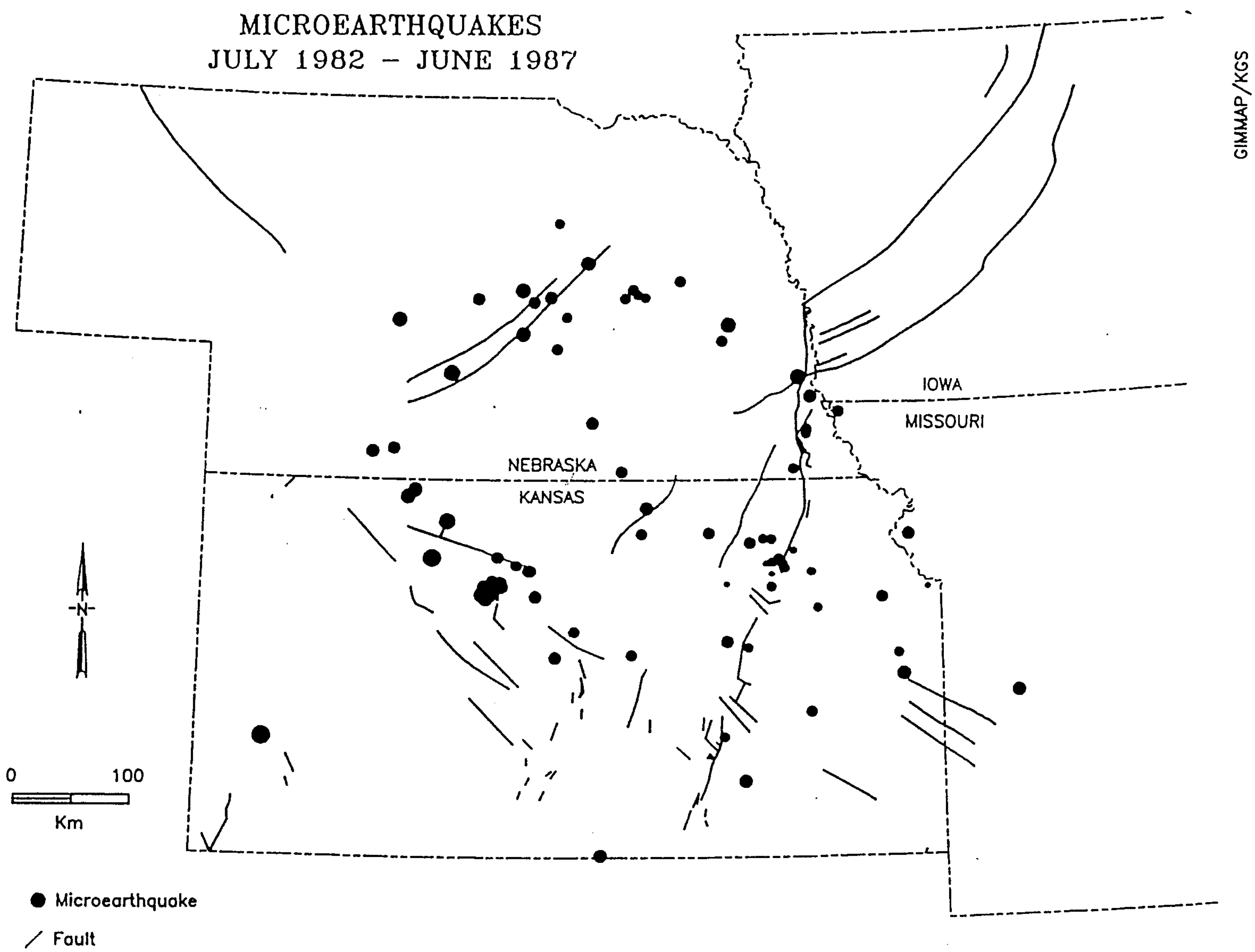
MICROEARTHQUAKES
JULY 1982 - JUNE 1987
IOWA
MISSOURI
NEBRASKA
KANSAS
GIMMAP/KGS
N
0
100
Km
Microearthquake
Fault

Figure 12.

(Explanation of Table 1)

The microearthquakes are listed in chronological order under the following headings:

DATE: year, month, day

ORIGIN: hour, minute, seconds, hundredths of seconds

LAT N: degrees, minutes, hundredths of minutes north

LONG W: degrees, minutes, hundredths of minutes west

DEPTH: calculated in kilometers or fixed at 5.00 km

MAG: duration magnitude calculated according to equation derived at Oklahoma Geological Observatory

NO: number of P- and S-arrivals used in hypocenter solution

GAP: largest azimuthal separation between stations measured from the epicenter

DMIN: epicentral distance in kilometers to nearest station

RMS: root-mean-square error of the time residuals

[$RMS = (\Sigma_i R_i^2/NO)^{1/2}$] where R_i is the observed seismic-wave travel time less the computed time at the i^{th} station

ERH: standard error of the epicenter in kilometers

[$ERH = (SDX^2 \& SDY^2)^{1/2}$] where SDX and SDY are the standard errors in latitude and longitude, respectively, of the epicenter

ERZ: standard error of depth in kilometers (asterisks are used if greater than 999 km). This is not a good estimate of depth uncertainty in a sparse network.

Q: quality of the event. In a dense network, values are A, B, C, D. Only C and D quality solutions are obtained because of the sparseness of the network. Q is based upon GAP, ERH, ERZ, DMIN, RMS, and NO.

M: Crustal model number. All of our locations use the same crustal model derived by Steeples and shown in Brown et al. (1983).

This table contains locations for all microearthquakes located with data from the Kansas network between 1 August 1977 and 1 May 1983.

Table 1. Earthquakes located by the KGS seismograph network in Kansas and Nebraska.

DATE	ORIGIN		LAT N	LONG W	DEPTH	MAG	NO	GAP	DMIN	RMS	ERH	ERZ	QM
770818	1034	25.22	41-24.88	98-28.09	5.00	2.5	9	249	289.2	1.14	26.2	21.2	D1
771201	13 4	34.21	40-18.53	100-22.01	5.00	2.29	7	197	326.6	.72	25.5	16.2	D1
771201	1322	37.82	40-18.65	100-17.78	1.23	2.38	6	197	321.2	.18	6.2	2.2	D1
771216	612	26.91	37- 9.88	97- 2.18	5.00	2.0	16	189	52.8	.54	3.0	2.8	D1
771220	756	39.37	37- 7.61	97- 1.80	5.00	2.34	11	189	48.6	.23	4.1	3.6	D1
780108	416	34.40	37- 4.59	97- 4.00	5.00	1.80	4	194	43.5	.05			C1
780111	2132	3.73	38-52.04	96-12.08	.02	1.64	7	162	43.9	.73	5.2	3.7	D1
780113	2015	42.32	39-31.71	96- 8.20	5.00	1.72	3	187	29.9	.53			D1
780127	1125	37.72	39-49.89	95-58.35	9.02	2.42	9	222	40.9	.16	1.3	13.4	D1
780203	025	48.32	39-41.49	100-22.91	7.69	2.40	6	186	307.5	.20	18.3	4.1	D1
780414	2327	38.32	39-48.86	96-23.68	1.22	1.9	5	240	55.4	.07	2.0	59.0	D1
780520	153	43.90	39-30.58	100-23.37	5.00	2.25	10	173	230.2	.98	31.4	14.0	D1
780522	428	34.81	39- 8.46	96-17.78	13.20	2.25	15	85	15.9	.36	1.1	2.8	C1
780914	8 6	18.27	40-52.55	100- 5.97	5.00	2.14	10	226	253.7	1.95	17.2	14.3	D1
781101	845	.26	39-50.27	97-20.61	9.68	1.69	10	255	48.4	.24	2.3	2.1	C1
781204	23 6	23.21	39- 8.27	100-27.30	5.00	2.30	8	184	240.1	.66	17.0	10.6	D1
781204	23 6	14.66	37-20.40	98-38.38	.52	2.2	8	166	84.3	1.50	5.6	2.1	D1
781210	1341	2.13	39-28.63	93-15.54	5.00	1.98	11	194	174.5	1.06	8.0	7.5	D1
790124	342	.87	39-37.13	96- 4.94	5.00	1.48	10	183	40.8	.34	1.9	25.6	D1
790210	1956	3.64	39-15.89	95-54.32	3.05	1.69	11	146	25.4	.88	4.0	44.9	D1
790225	1929	44.19	39- 8.02	92-40.30	5.00	1.83	11	184	195.2	.93	4.9	2.9	D1
790309	1147	43.51	37- 8.43	97-10.03	1.24	1.70	15	95	52.6	.83	2.9	3.8	D1
790309	1243	18.79	37- 9.63	97-10.61	1.49	1.82	20	96	55.0	1.21	3.6	4.2	D1
790408	2246	10.42	40-58.16	98-33.86	.67	2.42	12	176	114.3	.87	8.8	4.0	D1
790603	5 6	22.10	39-26.65	97-47.32	12.97	2.16	16	120	9.6	.43	2.3	1.5	C1
790606	1616	21.83	40- 8.39	100-22.00	1.00*	2.36	9	121	24.2	.60	3.1	6.0	D1
790612	1113	11.90	40-24.34	96- 3.27	2.13	1.8	10	160	5.6	.34	2.3	9.3	C1
790615	5 8	23.60	39-50.41	97-13.22	5.00	1.88	10	253	66.2	.66	5.3	7.7	D1
790625	730	22.46	38- .96	97- .34	2.09	1.59	12	178	32.6	.60	2.4	3.5	D1
790626	13 4	10.24	39-17.78	96- .99	8.94	2.03	12	84	16.2	.43	1.6	4.1	C1
790630	2046	41.35	39-56.20	97-16.46	5.00	3.11	10	139	60.7	.16	1.3	1.7	C1
790630	2110	7.28	39-54.51	97-17.54	5.00	1.38	8	235	57.3	.39	3.6	8.2	D1
790701	1959	34.83	39-53.84	97-16.72	5.00	2.03	11	233	57.1	.53	3.4	9.2	D1
790714	1832	26.83	39-31.54	99-15.35	12.65	2.10	13	180	81.4	.48	4.5	3.3	D1
790716	0 3	48.17	40- 9.65	100-17.58	5.00	2.7	13	168	24.4	.68	5.6	4.4	D1
790716	134	20.57	40-11.47	100-18.11	5.00	2.45	13	176	21.3	.44	3.2	2.6	C1
790716	527	1.44	40-11.45	100-20.01	9.06	1.29	5	187	22.3	.04	.7	3.5	C1
790716	6 8	9.85	40-11.37	100-20.85	11.54	1.47	6	192	23.0	.04	.4	1.3	C1
790716	7 5	56.66	40-13.07	100-13.60	5.00	1.09	3	153	17.3	.32			D1
790724	416	46.00	40-10.78	100-25.71	.10	2.17	4	217	27.7	.20			C1
790724	8 4	46.28	40-27.96	99-37.37	.88	1.9	7	224	52.1	.73	8.6	6.9	D1
790802	1046	32.55	38-55.78	96-33.76	18.22	2.20	12	115	34.6	.35	1.2	3.8	C1
790802	416	21.67	40-10.42	100-21.46	.86	2.5	10	261	28.0	.32	22.0	12.7	D1
790813	11 9	47.66	40- 6.80	100-30.12	1.33	1.7	5	234	21.2	.86	18.3	*****	D1
790814	2359	31.35	40-10.39	100-20.59	3.96	1.5	6	188	24.5	.22	1.3	16.2	D1
790815	645	53.84	40- 8.68	100-20.35	1.06	1.5	6	181	25.4	.15	1.0	1.7	C1
790815	16 7	7.18	40- 8.49	100-26.43	1.43	1.3	5	216	23.6	.14	3.5	287.6	D1
790831	8 0	11.72	40- 8.32	100-20.21	1.45	2.2	5	180	24.9	.32	4.8	677.0	D1

790909	0 0	22.21	39-23.46	95-53.52	5.00	1.52	9	122	30.1	.37	1.6	5.4	C1
791019	1617	25.84	37- 3.64	98-36.43	5.14	1.97	7	146	62.7	.45	5.7	9.2	D1
791019	2112	28.07	37- 5.39	98-35.30	5.00	1.78	11	154	66.0	.91	5.1	7.8	D1
791119	458	43.41	40-14.86	100- 2.76	13.61	1.58	4	271	20.7	.44			D1
791129	22 2	31.25	40- 9.78	100-21.46	1.29	1.9	6	169	4.9	.14	.7	1.2	B1
791207	1417	8.23	39-41.66	97-37.15	.19	2.01	6	245	22.2	.42	3.9	2.0	D1
791215	730	15.56	37- 5.43	98-28.25	.46	1.7	6	157	74.3	.45	2.0	14.3	D1
800211	545	44.47	39-56.06	97-18.48	1.02	2.1	8	190	56.1	.41	2.5	4.2	D1
800309	545	50.00	38-16.50	96-45.40	8.09	1.70	16	132	42.9	.51	1.8	3.9	D1
800309	922	43.97	38-16.23	96-43.77	5.00	1.62	14	129	41.0	.43	1.4	2.9	C1
800321	9 9	56.41	39-55.07	95-11.95	5.00	1.57	10	282	28.5	.21	1.9	2.0	C1
800326	1011	57.32	39-10.51	99- 8.32	17.83	1.71	14	206	114.7	.98	6.8	3.0	D1
800326	2256	58.32	39-58.85	95- 9.89	7.06	1.89	7	215	34.6	.05	.6	.9	C1
800416	713	21.55	39-54.36	97-16.27	5.00	1.64	16	181	56.2	.59	2.5	3.6	D1
800426	1421	48.50	40-43.98	99-43.91	5.00	2.22	12	243	82.5	.99	12.1	15.2	D1
800629	1614	31.32	38-56.57	95-18.48	5.00	1.80	15	185	84.9	.95	4.1	5.0	D1
800630	1 0	22.72	38-52.04	96-52.52	13.74	2.45	13	102	26.5	.36	1.5	6.9	C1
800810	1010	1.52	36-42.00	99- 8.87	32.39	2.14	15	241	.2	.94	12.9	4.5	D1
800813	550	14.64	41-41.51	96-57.63	5.00	2.1	10	260	93.2	.66	4.8	6.6	D1
800907	022	33.40	39-35.35	97-42.88	8.30	1.5	8	286	9.0	.37	4.5	3.6	D1
801109	1453	5.86	39-15.89	95-57.20	12.88	1.0	8	189	21.2	.31	7.8	4.4	D1
801122	334	9.68	36-32.36	98- 9.41	2.84	2.1	22	100	90.3	1.26	3.8	5.0	D1
810217	553	2.84	39-23.01	98-44.24	8.48	1.8	8	325	89.3	.44	7.3	9.1	D1
810313	1242	15.77	40-53.65	99-41.11	.26	2.4	8	214	227.8	.52	8.9	3.6	D1
810320	5 9	48.17	40-10.31	100-19.60	1.75	1.9	5	177	4.5	.09	.2	1.5	C1
810420	1818	13.50	41- 2.92	97-49.64	5.00	2.4	11	176	119.1	.67	5.7	7.0	D1
810530	9 7	10.35	39-21.66	94-51.62	.46	2.0	17	230	73.4	.43	2.5	1.0	D1
810620	516	52.16	38-44.18	98-20.38	8.39	1.8	13	184	68.4	.70	4.7	7.5	D1
810626	1855	2.07	41-31.75	97-39.06	5.00	2.7	17	256	76.4	.71	4.6	5.7	D1
810708	641	15.45	39- 4.04	96- 4.72	5.00	1.5	9	165	24.1	.29	2.0	12.4	C1
810717	1241	57.77	41-34.06	97-18.80	5.00	1.9	5	197	125.5	.31	3.0	6.1	D1
810801	158	44.50	38-20.54	97-55.84	10.00	2.7	14	158	73.5	.54	3.1	3.8	D1
811009	2154	25.58	41-15.83	98-41.88	5.00	2.7	21	205	142.2	.60	4.6	5.3	D1
811127	1 8	26.13	37- 2.85	98-50.92	5.00	2.2	14	127	47.0	.78	4.7	7.2	D1
811208	620	41.99	40-26.83	99-44.61	5.00	2.2	11	230	62.6	.74	7.0	6.5	D1
811217	544	53.82	36-22.88	97-37.47	9.99	2.4	15	238	138.0	.41	3.0	2.1	D1
820130	10 8	59.00	37-55.75	96-47.80	5.00	1.4	10	149	17.2	.31	3.4	11.6	C1
820224	2035	25.48	37-46.53	97- 8.73	6.92	2.2	20	184	30.9	.46	2.7	2.5	D1
820311	1819	57.05	39-15.41	99-21.39	8.84	1.9	9	218	91.0	.70	10.9	4.1	D1
820315	658	25.44	36-55.18	98-10.33	5.00	1.9	9	118	90.3	1.06	8.4	12.7	D1
820327	1957	23.61	38-53.32	95-58.64	5.00	1.6	8	136	45.8	.33	1.9	34.3	C1
820328	8 9	37.07	38-57.67	95-52.44	5.00	1.2	8	254	43.8	.46	4.9	46.0	D1
820406	012	59.98	39-30.58	97-42.88	5.00	1.4	8	288	.2	6.07	29.1	22.0	D1
820413	7 6	4.49	39-32.31	94-32.62	5.00	2.0	9	297	79.0	.23	2.4	1.8	C1
820424	1635	37.30	39-17.62	96-11.03	7.98	1.0	12	124	3.6	.28	1.2	.9	B1
820603	1420	50.20	40-10.91	96-35.12	4.68	2.2	20	118	24.2	.82	3.1	6.2	D1
820607	1726	26.10	37-55.74	96-58.43	5.00	1.5	6	226	23.3	.77	12.9	37.4	D1
820721	2141	35.77	38- 5.93	96- 9.00	2.28	2.58	23	117	41.3	.33	1.0	1.5	C1
820722	330	56.27	37- 9.29	98-32.04	5.65	2.29	9	155	74.5	.80	6.0	9.7	D1
820827	1419	25.39	40- 5.67	95-57.96	5.00	1.6	10	269	51.6	.19	1.6	3.3	C1
820903	1055	20.54	38-47.43	98-53.55	10.86	2.5	12	197	113.3	.21	2.0	1.9	C1
820906	1445	59.10	39-20.77	96-18.04	4.27	1.6	6	140	12.7	.22	2.8	15.3	C1
821026	044	7.76	39-30.27	96-31.52	17.04	1.8	12	159	38.8	.19	.9	3.1	C1
821223	222	.79	40-49.06	99-32.98	5.00	2.5	12	178	74.9	.33	6.0	5.7	D1

830209	1610	23.93	38-36.34	97-43.48	10.18	1.68	20	216	40.0	.20	.9	.9	C1
830212	1624	3.22	41-23.84	99-17.52	8.88	1.82	9	297	31.1	.31	3.3	2.4	D1
830226	624	58.34	41-22.45	98-43.12	5.00	1.82	6	295	109.4	.31	4.5	2.7	D1
830303	821	35.72	38-36.52	95- 3.08	5.00	1.47	8	276	50.4	.58	11.2	31.5	D1
830521	2151	1.81	38-47.47	98-16.92	5.00	1.70	17	238	61.6	.93	5.1	4.1	D1
830524	146	40.79	40-12.76	100-21.20	5.00	1.98	18	175	.2	.62	4.1	1.8	D1
830620	222	36.31	41-28.30	97-42.42	5.00	1.74	10	172	24.5	.63	3.3	12.4	D1
830626	1241	56.77	40-47.06	96- 1.15	8.85	2.43	18	205	37.5	.51	3.1	2.1	D1
830712	2030	41.29	39-14.82	96-18.53	.38	0.83	8	173	9.6	.17	1.2	.5	C1
830802	649	43.18	40-20.81	95-56.89	5.00	1.35	7	175	12.6	.36	3.6	14.0	C1
830824	9 2	14.94	39- 8.66	96-18.63	5.00	1.48	13	126	16.3	.39	1.2	3.9	C1
830907	1856	34.93	38-35.26	98-28.60	5.00	2.02	14			1.00	5.2	4.8	
831029	1038	56.18	40- 4.92	96- 4.76	5.00	1.55	10	115	40.9	.31	1.2	6.7	C1
831116	547	45.55	42-40.86	100-36.76	5.00	2.19	9			.57	10.3	.35	
831201	1123	50.53	41-13.90	100- 6.71	5.00	2.28	14			1.07	11.0	5.2	
831209	2059	47.52	39-24.20	92-31.30	5.00	1.82	8			.33	10.2	10.2	
831225	1445	29.96	39- 4.02	98-40.73	5.00	1.93	15	257	94.1	.40	2.4	2.0	D1
840107	1945	34.90	40- 3.99	97-49.64	5.00	1.75	10	155	49.4	.52	2.4	9.4	D1
840113	2137	58.90	39-22.44	96-14.20	.83	1.73	5	112	12.7	.01	.2	.4	C1
840127	333	28.12	41- .60	98-28.52	9.53	1.69	10	169	51.1	.86	5.7	93.1	D1
840203	2141	55.68	39-31.70	96-18.80	1.50	1.44	5	234	31.0	.09	1.7	196.3	D1
840812	6 0	50.17	38-42.02	96-46.89	19.83	1.89	12	111	46.0	.32	1.6	1.8	C1
840828	424	40.29	38-16.42	93-50.92	5.00	2.07	8	146	312.1	.30	5.0	2.6	D1
841023	1032	19.25	38- 8.76	95-55.84	5.00	1.7	11	47	269.1	.36	3.4	7.2	D1
841110	333	21.29	40-30.60	95-36.73	5.00	1.70	15	269	35.1	.57	3.8	4.6	D1
841204	1718	57.67	39-52.06	99-58.55	5.00	2.3	9	47	195.1	.30	4.7	6.7	D1
841218	1612	47.70	41-33.57	97-11.01	5.00	1.8	8	216	17.3	.47	4.3	1.9	D1
850208	913	55.43	40-22.84	95-56.58	5.00	1.6	7	190	9.7	.35	2.7	6.6	D1
850302	12 5	30.64	39-34.89	96-55.38	9.13	1.8	9	161	27.8	.32	2.4	6.4	C1
850405	5 8	36.50	39-34.62	97-37.31	10.68	1.67	10	120	11.0	.36	2.3	4.1	C1
850415	1429	21.51	40-26.24	98- 6.66	8.64	1.88	9	162	16.5	.36	2.2	3.2	C1
850425	710	17.52	39-20.05	96-21.64	5.00	1.04	6	199	16.0	.15	2.0	8.4	D1
850426	849	14.98	39-34.89	96-56.40	5.00	1.18	5	207	28.8	.07	5.4	35.6	D1
850601	420	3.26	39- 8.59	99- 9.54	10.18	2.12	14	287	131.2	.34	2.6	1.4	D1
850601	1021	9.33	39- 6.09	99-12.36	14.73	1.70	11	298	136.5	.29	3.0	1.3	D1
850601	1242	54.12	39- 8.31	99-11.09	11.15	2.26	13	288	133.4	.34	2.9	1.7	D1
850603	913	59.21	40-14.47	100- 8.11	5.00	1.79	9	277	155.7	.25	4.6	22.2	D1
850620	17 8	37.80	39- 9.91	96-45.45	5.00	0.80	5	140	24.6	.23	3.0	8.9	D1
850710	4 5	6.66	38-58.34	95-51.25	2.02	1.28	8	133	44.0	.25	1.23	25.5	C1
850718	1553	49.01	41-24.66	97-34.95	.25	1.42	5	206	19.2	.11	2.3	1.1	C1
850720	1151	32.54	41-28.12	98-50.27	1.50	2.28	12	241	19.7	.58	3.4	2.7	D1
850722	14 5	44.33	41-26.04	97-39.53	5.00	1.43	8	156	22.6	.44	6.3	29.1	D1
850729	2253	22.65	39-23.30	99- 3.88	5.00	1.88	11	252	117.2	.64	4.5	4.6	D1
850806	331	49.29	39- 4.89	99- 8.44	17.16	2.27	14	268	131.9	.36	3.1	1.7	D1
850806	827	35.12	39- 8.86	99- 3.87	5.00	2.19	11	263	128.3	.60	4.6	3.7	D1
850806	21 8	11.54	39- 3.13	99-10.89	13.74	2.33	15	240	136.4	.21	1.3	.8	C1
850809	1810	32.92	39- 4.88	99-12.96	10.76	2.48	14	270	138.0	.32	2.9	1.4	D1
850914	1732	35.47	41-11.84	96-43.25	19.48	2.28	13	110	7.2	.20	1.1	.8	B1
851001	329	14.62	41- 4.33	96-47.28	5.00	1.74	9	183	74.6	.34	2.1	3.1	D1
851021	1931	5.42	39-40.43	99-33.94	8.90	2.45	15	245	160.2	.54	3.7	2.7	D1
851101	8 8	45.38	39-20.25	96-12.08	16.05	1.53	7	130	8.2	.56	4.1	3.5	C1
851122	342	33.14	39-16.54	98-44.49	5.00	2.10	13	246	92.3	.59	3.8	4.9	D1
851226	013	48.64	41-15.53	98-22.58	2.97	1.51	6	211	47.4	.77	13.0	40.0	D1
860202	11 4	45.87	41-24.76	98-32.62	9.94	1.88	7	191	35.0	.49	4.6	5.7	D1

860304	751	3.19	39-33.37	94-55.50	5.00	1.93	9	264	56.1	.16	1.8	3.9	C1
860313	2021	36.29	38-26.39	95- .47	5.00	2.07	12	319	69.5	.35	2.8	2.1	D1
860602	4 4	6.46	39-22.85	99-42.05	16.03	3.0	26	103	171.8	.41	2.1	3.6	D1
860604	2237	21.99	37-35.32	96-35.14	5.00	2.06	9	145	27.6	.54	5.9	7.7	D1
860728	2215	7.04	39-15.89	95-54.82	5.00	1.43	12	227	24.7	.51	4.2	9.6	D1
860901	224	2.64	39-17.84	96-10.89	8.77	1.57	10	125	4.1	.22	1.0	1.7	B1
860924	734	58.52	40-37.80	95-54.09	5.00	2.02	9	254	22.6	.35	4.1	3.1	D1
860927	934	2.24	39-55.29	99-54.64	.10	2.22	8	270	174.6	.47	6.9	2.5	D1
861020	432	49.57	37-55.86	101-21.81	.44	3.0	17	109	239.5	.63	2.6	2.0	D1
861008	1110	31.74	39-11.54	99- 6.82	12.41	1.90	12	293	125.6	.63	5.7	2.5	D1
861009	1541	29.10	39-10.96	99- 1.99	.01	1.90	9	291	119.5	.34	11.5	3.9	D1
861011	817	35.40	39- 8.91	99-11.48	5.00	1.87	9	297	133.6	.43	5.2	3.4	D1
861105	541	48.44	38-39.76	96-32.99	5.00	1.41	8	293	57.5	.33	3.3	9.3	D1
861109	9 5	7.24	39-26.44	96- 5.53	7.51	0.96	7	100	21.8	.22	2.2	7.6	C1
861125	639	26.53	39- 6.53	99- 8.60	12.83	2.28	11	267	131.1	.66	6.8	3.2	D1
861209	1111	45.53	39- 8.79	99- 1.53	5.00	2.13	12	180	120.1	.68	5.0	7.2	D1
861231	2157	4.95	37- .97	98- 1.00	5.00	2.02	10	133	106.7	.49	2.5	3.3	D1
870109	1852	3.80	39-46.82	97-34.34	5.00	2.03	16	124	32.6	.41	1.4	2.2	C1
870124	1035	24.03	41-41.37	98- 9.45	6.78	2.23	9	228	63.1	.28	3.4	1.8	D1
870202	9 1	25.13	41- 7.71	98-49.92	3.11	2.18	9	184	21.9	.29	2.1	1.8	C1
870210	2014	56.05	39- 7.38	94-44.59	.83	0.80	7	282	40.8	.58	16.0	16.1	D1
870213	233	45.32	37-56.98	96-47.50	5.00	1.55	4	181	19.5	.02			C1
870216	229	34.67	41-24.16	97-47.32	5.00	1.52	6	160	33.8	.15	1.3	2.9	C1
870219	1426	44.46	39-32.19	96-23.54	13.76	1.42	10	107	33.0	.20	1.1	4.3	C1
870315	1732	35.18	42- .44	98-27.73	5.00	1.62	7	274	87.2	.28	3.3	2.9	D1
870323	343	2.94	39-19.34	98-52.50	5.00	1.77	9	248	117.4	.48	5.3	4.2	D1
870610	1858	54.51	39-42.35	97-55.46	4.03	1.58	4	219	28.5	1.54			D1

Table 2

EVENTS RECORDED BY THE KGS DIGITAL EARTHQUAKE RECORDING SYSTEM

#	DATE	ORIGIN	LOCATION		GEOGRAPHIC	MAG
1	85-02-10	09:13:54.2	40.449	95.899	Nemaha Co., Ks.	1.6
2	85-03-02	12:05:30.9	39.588	96.898	Riley County, Ks.	1.80
3	85-06-01	04:20:03.3	39.143	99.159	Ellis County, Ks.	2.12
4	85-06-01	10:21:09.3	39.102	99.206	Ellis County, Ks.	1.70
5	85-06-01	12:42:54.1	39.141	99.181	Ellis County, Ks.	2.26
6	85-07-20	11:51:32.5	41.469	98.838	Valley Co., Ne.	2.28
7	85-08-06	03:31:49.3	39.082	99.141	Ellis County, Ks.	2.27
8	85-08-06	08:27:35.1	39.148	99.065	Ellis County, Ks.	2.19
9	85-08-06	21:08:11.5	39.052	99.182	Ellis County, Ks.	2.33
10	85-08-09	18:10:32.9	39.081	99.216	Ellis County, Ks.	2.48
11	85-09-06	22:17:02.8	35.811	93.123	NW Arkansas	3.6
12	85-09-14	17:32:35.5	41.197	96.721	Saunders Co., Ne.	2.28
13	85-09-18	15:54:04.5	33.547	97.034	Central Texas	3.3
14	85-10-01	03:29:14.6	41.072	96.788	Saunders Co., Ne.	1.74
15	85-10-21	19:31:05.4	39.683	99.531	Phillips Co., Ks.	2.45
16	85-11-22	03:42:33.1	39.276	98.742	Osborne Co., Ks.	2.10
17	86-03-13	20:21:36.3	38.440	95.008	SW Miami Co., Ks.	2.07
18	86-05-24	12:48:12.5	36.605	89.906	New Madrid, Mo.	3.4
19	86-05-25	07:13:22.2	43.916	98.284	South Dakota	3.4
20	86-06-02	04:04:06.3	39.398	99.714	Graham Co., Ks.	3.0
21	86-07-12	08:19:37.9	40.544	84.354	Ohio	4.5
22	86-08-26	16:41:24.2	38.340	89.790	S Illinois	3.7
23	86-09-27	09:34:02.2	39.922	99.911	Norton Co., Ks.	2.22
24	86-10-20	04:32:49.6	37.931	101.364	Kearny Co., Ks.	3.0
25	86-11-25	06:39:26.5	39.109	99.143	Ellis County, Ks.	2.28
26	86-12-21	17:32:58.1	35.150	96.680	Oklahoma	2.8
27	87-01-09	18:52:03.8	39.780	97.572	Republic Co., Ks.	2.03
28	87-01-24	16:08:17.0	35.830	98.090	Oklahoma	3.1
29	87-03-21	00:49:28.6	43.170	98.702	South Dakota	2.2
30	87-03-23	03:43:02.9	39.322	98.875	Osborne Co., Ks.	1.77
31	87-06-10	23:48:54.8	38.713	87.954	Southern Indiana	5.1
32	87-06-13	21:17:13.1	36.590	89.660	New Madrid, Mo.	4.1

Table 3. This table contains station locations for all stations used during the life of the network. Most of the stations are not operated by the KGS. The crustal model is listed at the end of the station locations.

STN	LAT	LONG	ELV
BEK	3915.79N	9611.98W	349
EMK	3826.79N	9619.03W	307
HWK	3948.13N	9529.79W	320
LAK	39 2.78N	9512.27W	326
MLK	39 6.36N	9653.54W	386
TCK	3923.09N	9643.35W	377
EDK	3746.43N	9647.70W	418
SNK	3857.18N	9736.18W	407
CNK	3930.48N	9742.78W	465
MEO	3446.96N	9835.11W	458
RSOZ	3734.16N	96 8.43W	340
ALQ	3456.55N	10627.45W	1849
JHN	4026.82N	96 1.05W	329
CUN	4128.73N	9722.80W	466
MKN	4022.44N	10013.50W	730
DTN	41 1.30N	97 2.15W	465
SGN	41 3.95N	9613.12W	348
HMN	4017.18N	9650.13W	368
TUL	3554.00N	9547.55W	256
WLO	34 3.80N	9722.18W	284
SIO	3544.78N	9618.42W	323
CRO	34 9.00N	9433.33W	302
ACO	3641.90N	99 8.77W	521
PCO	3641.47N	9658.68W	331
RLO	3610.02N	95 1.52W	363
QMO	3453.57N	9918.42W	479
MRO	3550.13N	9713.59W	964
MZO	36 7.90N	9518.00W	182
RRO	3527.42N	9821.51W	482
GBO	3551.15N	9511.06W	302
JRTX	3256.04N	10057.18W	804
FVM	3759.04N	9025.56W	0
TYS	3830.90N	9034.08W	195
GOL	3942.02N	10522.27W	2359
RFI	4041.35N	9533.97W	308
TPI	4114.07N	9532.10W	350
PHI	4149.62N	9550.75W	384
ESI	4134.77N	95 9.02W	376
CAI	41 2.05N	9449.90W	357
MRN	40 7.19N	10025.90W	793
NNKA	3953.13N	100 2.22W	756
NRTK	3953.13N	100 2.22W	756
SCN	40 7.99N	10020.60W	783
SHN	4010.47N	10019.89W	766
QZO	3454.31N	9918.32W	488
BHO	3418.48N	9452.04W	143
OCO	3531.44N	9728.44W	0

SHAN	4012.66N	10021.10W	0
SHBN	4011.45N	10020.91W	0
SHCN	40 9.60N	10026.00W	0
SHDN	40 9.91N	10022.64W	0
SHEN	40 9.65N	10020.86W	0
SHFN	4010.08N	10017.79W	0
SHGN	40 8.81N	10023.15W	0
SHHN	40 7.81N	10025.35W	0
BENE	4013.00N	9636.15W	1300
PCNE	4132.35N	9725.65W	1580
LCNE	4118.50N	9856.32W	2200
CCNE	4030.22N	9756.20W	1735
WHNE	4114.17N	9639.15W	1250
JHN	4026.80N	96 1.12W	1100
RSSD	44 7.22N	104 2.17W	2060
ATO	3547.53N	98 7.17W	0
BDW	4246.57N	10934.10W	2190
LTX	2920.03N	10340.02W	1013
VVO	3520.21N	9544.24W	224
RSON	5051.53N	9342.13W	335

CRUSTAL MODEL 1

VELOCITY	DEPTH
2.400	.000
4.500	.526
6.000	1.300
6.100	8.113
8.250	42.000

Table 4.

OPERATIONAL EFFICIENCY

KANSAS AND NEBRASKA EARTHQUAKE NETWORK

(July 1, 1983 - June 30, 1987)

	Total Station Days Down	Potential Station Days Up	% Efficiency
In Kansas:			
Belvue (BEK)	35.6	1461	97.6
Concordia (CNK)	41.4	1461	97.2
Eldorado (EDK)	32.8	1461	97.8
Emporia (EMK)	32.1	1461	97.8
Hiawatha (HWK)	37.2	1461	97.5
Lawrence (LAK)	12.2	1461	99.2
Milford Lake (MLK)	34.3	1461	97.7
Salina (SNK)	41.3	1461	97.2
Tuttle Creek (TCK)	37.6	1461	97.4
In Nebraska:			
Beatrice (BENE)	44.9	1461	96.9
Clay Center (CCNE)	26.8	1461	98.2
Johnson (JHN)	27.7	1461	98.1
Loup City (LCNE)	18.2	1461	98.8
Platte Center (PCNE)	31.3	1461	97.9
Wahoo (WHNE)	23.6	1461	98.4
	Average Operational Efficiency		97.8%

APPENDIX A.

Kansas-Nebraska Seismicity, 1984

by Greg Hildebrand and Don W. Steeples
Kansas Geological Survey
Lawrence, KS 66046

The Kansas Geological Survey operates a seismic network of fifteen single component, short period stations throughout eastern Kansas and eastern Nebraska. The network is operated under a contract with the U.S. Nuclear Regulatory Commission and is designed to monitor seismic activity in eastern Nebraska and eastern Kansas. A dense network of eight stations was also operated in the Sleepy Hollow oil field through 1984 near 40.2 N., 100.4 W. The Sleepy Hollow network was funded by the USGS and a NSF grant. The addition of digital acquisition capabilities to the Sleepy Hollow network made it possible to achieve better resolution on several of the 62 events located in 1984. Figure A1 shows the station locations on January 1, 1984. Operation of the Sleepy Hollow network ceased in late December, 1984.

Figure A2 shows cumulative microearthquake epicenters recorded since August, 1977. Four major microearthquake trends can be identified from this figure. One trend is associated with the Humboldt Fault Zone running south-southwesterly from near 40 N., 96 W. to near 37 N., 97 W. A second trend is nearly parallel to the first and is associated with the northwest flank of the Midcontinent Geophysical Anomaly, running south-southwesterly from near 40 N., 97.3 W. to near 37 N., 98.5 W. A third trend is generally associated with the Central Kansas Uplift, running from near 38 N., 98 W.northwesterly to the Sleepy Hollow area near 40.2 N., 100.4 W. The final trend runs northeastward across Nebraska from Sleepy Hollow to near 42 N.,97 W.

Table A1 shows locations and local duration magnitudes for events recorded in the Kansas-Nebraska network during 1984. A total of 10 events were recorded in Kansas and Nebraska in 1984 and no events are known to have been felt. The location of 62 events by the Sleepy Hollow Network are shown in Table A2, but are not included in Figure A2. All of the events were located using HYPO 71 (Lee and Lahr, 1975).

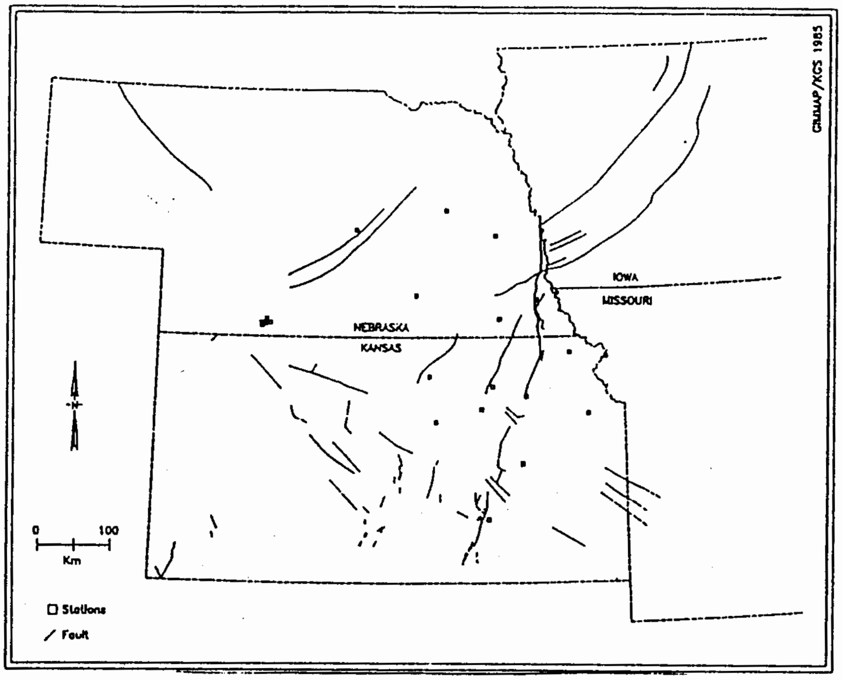

FIGURE A1. Seismograph stations in Kansas and Nebraska in January 1984. Sleepy Hollow stations are shown by the cluster of squares in southwestern Nebraska.

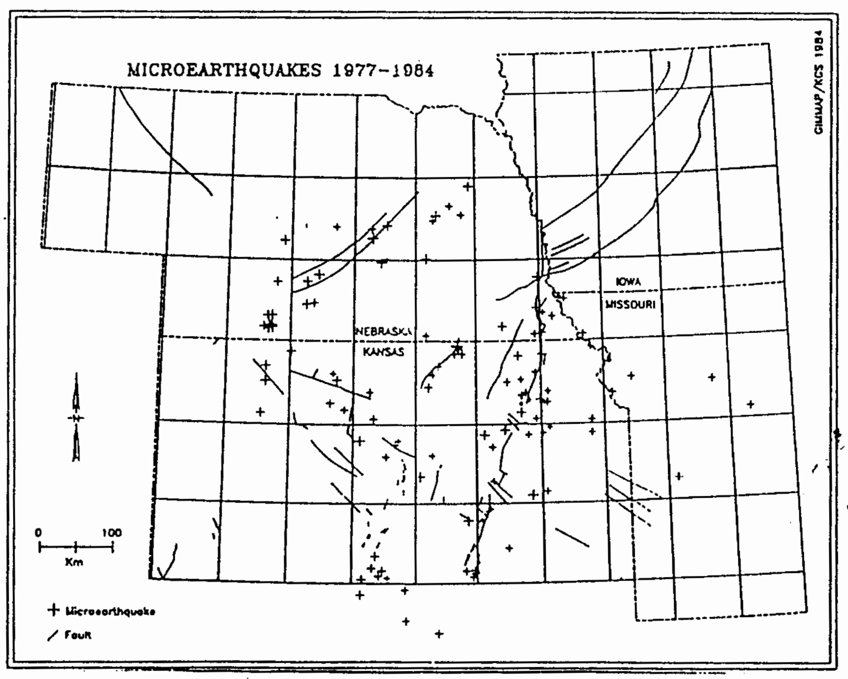

FIGURE A2. Microearthquakes located by Kansas seismograph network between August 1977 and December 1984, shown by size coded plus signs. The largest event had a magnitude of 3.3 Mn. The smallest events had magnitudes of about 1.0 (local duration scale).

EXPLANATION OF OF TABLES A1 AND A2

The microearthquakes are listed in chronological order under the following headings:

DATE: year, month, day

ORIGIN: hour, minute, seconds, hundredths of seconds

LAT N: degrees, minutes, hundredths of minutes north

LONG W: degrees, minutes, hundredths of minutes west

DEPTH: calculated in kilometers or fixed at 5.00 km

MAG: duration magnitude calculated according to equation derived at Oklahoma Geological Observatory

NO: number of P- and S- arrivals used in hypocenter solution

GAP: largest azimuthal separation between stations, measured from the epicenter

DMIN: epicentral distance in km to nearest station

RMS: root-mean-square of the time residuals

ERH: standard error of epicenter in kilometers

ERZ: standard error of depth in kilometers, (asterisks are used if greater than 999 km). This is not a good estimate of depth in a sparse network.

Q: quality of the event. In a dense network, values are A, B, C, D. Only C and D solutions are obtained because of the sparseness of the network. Q is based upon GAP, ERH, ERZ, DMIN, RMS and NO.

TABLE A1. Kansas and Nebraska earthquakes, 1984

DATE	ORIGIN	LAT N	LONG W	DEPTH	MAG	NO	GAP	DMIN	RMS	ERH	ERZ	QM
840107	1945 34.90	40- 3.99	97-49.64	5.00	1.75	10	155	49.4	.52	2.4	9.4	D1
840113	2137 58.90	39-22.44	96-14.20	.83	1.73	5	112	12.7	.01	.2	.4	C1
840127	333 28.12	41- .60	98-28.52	9.53	1.69	10	169	51.1	.86	5.7	93.1	D1
840203	2141 55.68	39-31.70	96-18.80	1.50	1.44	5	234	31.0	.09	1.7	196.3	D1
840812	6 0 50.17	38-42.02	96-46.89	19.83	1.89	12	111	46.0	.32	1.6	1.8	C1
840828	424 40.29	38-16.42	93-50.92	5.00	2.07	8	146	312.1	.30	5.0	2.6	D1
841023	1032 19.25	38- 8.76	95-55.84	5.00	1.7	11	47	269.1	.36	3.4	7.2	D1
841110	333 21.29	40-30.60	95-36.73	5.00	1.70	15	269	35.1	.57	3.8	4.6	D1
841204	1718 57.67	39-52.06	99-58.55	5.00	2.3	9	47	195.1	.30	4.7	6.7	D1
841218	1612 47.70	41-33.57	97-11.01	5.00	1.8	8	216	17.3	.47	4.3	1.9	D1

TABLE A2. Earthquakes located by the sleepy Hollow, Nebraska, seismic network, 1984

DATE	ORIGIN	LAT N	LONG W	DEPTH	MAG	NO	GAP	DMIN	RMS	ERH	ERZ
*840101	1453 0.51	40- 9.97	100-22.59	1.53	-0.29	6	121	0.1	0.01	0.1	0.1
*840101	1852 12.21	40- 9.64	100-23.65	0.87	-0.11	7	124	1.5	0.02	0.1	0.1
*840202	845 13.59	40-10.03	100-22.65	1.91	-0.32	6	143	0.2	0.01	0.1	0.1
*840203	1548 5.92	40- 9.79	100-22.06	2.23	-0.71	5	136	0.8	0.00	0.1	0.1
*840311	835 0.79	40- 9.92	100-23.73	2.00	-0.93	3	191	1.5	0.00		
*840315	028 32.17	40-10.75	100-21.56	1.21	0.07	7	144	1.6	0.01	0.1	2.3
*840331	2350 0.31	40- 9.79	100-21.84	3.19	-0.65	5	141	1.2	0.01	0.2	0.5
840406	300 35.43	40-10.38	100-22.20	1.71	-0.26	5	162	1.0	0.00	0.0	0.0
840408	2130 52.77	40-10.24	100-20.58	3.19	-0.18	5	139	3.0	0.05	0.8	2.8
*840425	247 0.58	40-10.07	100-22.83	2.00	-0.19	6	148	0.4	0.01	0.2	0.2
*840425	252 0.66	40-10.16	100-22.86	2.00	-0.19	4	194	0.6	0.00		
*840425	1432 0.34	40-10.93	100-21.31	1.94	0.08	5	141	1.1	0.01	0.1	0.2
840501	1423 2.03	40-11.73	100-21.74	2.60	-0.02	6	273	1.3	0.06	1.2	1.2
*840621	353 46.45	40-10.45	100-21.22	0.92	0.14	7	124	1.9	0.08	0.6	0.3
*840621	1108 26.00	40-10.36	100-21.21	2.65	0.76	6	128	2.1	0.02	0.3	0.7
840628	809 1.63	40-10.74	100-21.00	2.94	-0.09	6	121	1.3	0.02	0.2	0.5
840628	819 35.38	40-15.21	100-20.06	1.17	-0.55	4	322	4.9	0.22		
840628	819 41.95	40-10.83	100-20.72	1.16	-0.23	7	118	3.2	0.05	0.3	78.3
840720	631 47.10	40- 8.68	100-24.78	2.00	-0.44	3	332	3.8	0.05		
840724	1731 8.94	40-10.25	100-21.76	0.71	-0.56	4	188	1.4	0.03		
840827	1506 50.99	40-12.85	100-16.84	2.00	-0.40	3	312	5.4	0.39		
840828	1508 55.60	40- 9.65	100-23.30	1.48	-0.34	8	169	1.1	0.06	0.8	1.1
840905	539 29.30	40-11.48	100-20.65	0.99	0.19	6	140	0.4	0.04	0.5	0.2
840914	1233 21.94	40-11.79	100-21.08	2.00	-0.12	3	356	4.1	0.16		
840915	231 44.32	40-11.07	100-23.39	2.00	-0.28	3	338	2.4	0.00		
840915	305 20.31	40-11.01	100-23.85	2.00	-0.16	3	334	2.7	0.00		
840917	318 28.83	40-10.73	100-23.26	0.98	-0.28	7	234	1.8	0.04	0.7	0.2
840917	1830 36.64	40- 9.52	100-23.16	3.39	0.06	6	162	1.0	0.03	0.5	0.4
840919	1323 16.89	40- 9.93	100-23.71	3.18	0.10	10	187	1.5	0.07	0.7	0.8
840921	1113 7.23	40- 9.75	100-23.56	3.24	0.20	7	195	1.3	0.07	1.2	1.1
840922	912 43.35	40-10.27	100-21.50	2.18	-0.48	7	134	1.7	0.14	1.7	2.4
*840922	1357 9.17	40-11.28	100-20.70	2.97	-0.12	5	132	0.4	0.06	1.1	2.1
840924	1714 56.91	40- 8.17	100-23.60	1.17	-0.36	5	223	1.3	0.08	1.3	5.2
840924	2208 35.27	40-10.01	100-25.50	2.00	-0.41	3	326	4.0	0.09		
840925	2026 55.40	40-10.01	100-23.86	4.10	0.10	7	210	1.7	0.05	1.4	0.9
840927	747 7.87	40-10.08	100-22.86	2.00	-0.56	3	197	0.4	0.05		
841001	2052 54.71	40-12.17	100-23.90	2.00	-0.79	4	304	4.5	0.20		
841004	918 19.54	40- 9.57	100-23.52	2.00	-0.43	3	247	1.4	0.03		
841013	1554 47.56	40-10.13	100-21.47	0.91	-0.45	5	133	1.7	0.01	0.2	0.1
841016	2300 21.33	40-10.92	100-21.41	1.27	0.07	7	145	1.2	0.02	0.2	0.9
841016	2305 54.76	40-10.79	100-20.78	1.25	0.19	8	116	1.2	0.04	032	2.9
841027	034 7.10	40- 9.96	100-22.93	3.40	-0.00	8	185	0.4	0.02	034	0.3
841031	333 54.10	40-10.38	100-24.13	0.09	-0.43	4	299	2.3	0.04		
841101	527 11.31	40-10.69	100-22.91	4.59	-0.56	4	274	1.5	0.00		
841113	1747 56.32	40-10.57	100-21.65	0.74	-0.58	5	164	1.9	0.15	2.2	0.9
*841125	1836 7.64	40-10.93	100-21.14	2.19	0.13	6	133	1.0	0.01	0.2	0.3
841126	1856 26.94	40-11.64	100-23.51	1.03	-0.60	4	247	3.4	0.02		

841127	1945	12.58	40-10.01	100-23.29	2.00	-0.56	3	237	0.9	0.18		
841128	516	5.99	40-11.25	100-22.74	2.00	-0.54	3	280	2.5	0.31		
841128	726	36.61	40-10.70	100-21.07	1.18	-0.16	7	122	2.7	0.06	0.4	91.0
841203	140	11.05	40-12.07	100-20.13	2.76	-0.69	6	192	1.6	0.11	1.7	2.1
841203	1423	33.26	40- 8.03	100-20.45	2.00	-0.04	3	248	4.1	0.00		
841203	1442	43.32	40- 6.12	100-18.07	2.00	-0.00	3	304	7.3	0.47		
841203	1444	47.49	40- 1.18	100-14.24	1.02	1.21	5	326	7.3	0.00	1.3	7.7
841204	1750	30.73	40- 9.87	100-22.35	2.27	0.26	7	109	0.4	0.01	0.1	0.2
841205	1254	10.48	40-11.61	100-21.51	2.00	-0.71	3	272	3.5	0.27		
841211	656	53.62	40- 9.12	100-21.37	2.00	-0.77	3	187	2.3	0.00		
841211	656	58.37	40- 8.91	100-23.19	2.00	0.36	3	219	0.2	0.09		
841214	425	36.53	40-10.83	100-24.87	3.07	-0.49	4	331	3.6	0.06		
841214	612	6.16	40- 9.71	100-23.84	2.07	-1.01	3	231	0.7	0.00		
*841214	1943	41.70	40- 9.98	100-21.89	1.54	0.35	7	110	1.1	0.02		
841220	024	24.91	40-11.41	100-20.54	2.00	-0.20	3	237	0.5	0.04		

* Location using digital data

APPENDIX B

KANSAS REFRACTION PROFILES

by
Don W. Steeples and Richard D. Miller

Kansas Geological Survey
The University of Kansas
Lawrence, Kansas 66046

ABSTRACT

Historically, refraction surveys have been conducted in hopes of mapping distinct layers within the earth. Refraction is a useful tool provided its limitations and the assumption that layers increase in seismic velocity with increasing depth are kept in mind. A traditional reversed refraction profile was conducted along a 500-km-long east-west line extending from Concordia, Kansas, to Agate, Colorado. Analysis of the data showed an average crustal velocity of 6.1 km/sec and an average upper-mantle P_n phase velocity 8.29 km/sec with a Moho depth calculated to be 38 km on the eastern end and 48 km on the western end. Some evidence suggests velocities as high as 7.2 km/sec in the crust at various locations along the survey line. The strong east to west regional gravity gradient of -0.275 mgal/km supports the seismically drawn conclusion of a thinning of crust in north-central Kansas. In order to supplement the data from this refraction survey, we took advantage of the Kansas earthquake seismograph network. A crustal study using earthquakes as energy sources and a regional earthquake network as seismometer locations resulted in a crustal-velocity model that will improve local earthquake locations. A large anomalous body in the upper mantle/lower crust, assumed to be related to the Precambrian-aged Midcontinent Geophysical Anomaly (MGA), resulted in early P-wave arrivals from refracted energy from the Moho recorded at Concordia, Salina, Tuttle Creek, and Milford. An omnidirectional positive P_n residual zone near El Dorado may be related to the Wichita geomagnetic low. Some evidence suggests the presence of a lower velocity material on the western and eastern flank of the MGA, possibly representing the Rice Formation. A P_n velocity of 8.25 km/sec 0.15 km/sec with the crust thinning from west to east and an apparent thinning from the north and from the south was determined from the 16 regional earthquakes studied. Crustal thickness from central Kansas through western Missouri seems to be relatively consistent.

INTRODUCTION

For regional geologic, geophysical, and tectonic studies, having some idea of gross characteristics of the deep crust is useful. Knowledge of the deep crust and upper mantle necessarily comes from indirect observations. Since the deepest borehole in Kansas extends only to about 3.5 km, geophysical observations made at or near the earth's surface must be used to infer geologic conditions at greater depths.

Methods used to model deep crustal structure in Kansas include seismic reflection (Brown et al., 1983; Serpa et al., 1984; Serpa et al., this volume), seismic refraction (Steeples, 1976), gravity and magnetics (Yarger 1983; Yarger et al., 1980), and studies using earthquake waves (Hahn, 1980; Hahn and Steeples, 1980; Steeples, 1982; Lui,1980; Miller, 1983). More direct information was obtained by examination of deep-crustal and upper-mantle xenoliths in kimberlites from Riley County by Brookins and Meyer (1974).

This paper is a presentation of more complete results of work by Steeples (1976) and an abbreviation of an M.S. thesis by Miller(1983). This paper is likely to be most useful to those interested in earthquakes and tectonics of the Midcontinent and to those interested in existing and planned deep seismic reflection surveys in Kansas.

GEOLOGIC SETTING

The area under investigation is contained within the Central Stable Region (Snyder, 1968, Fig. 1). The generalized continental crust is made up of a silicic upper layer covering a mafic lower layer (Pakiser and Zeitz, 1965). The stable environment of the Midcontinent shows a relatively thick crust (approximately 50 km) with lower crustal P-wave velocities about 6.7 km/sec generally representative of a gabbro. The upper mantle rocks show P-wave velocities in excess of 8.0 km/sec with relatively high density (Pakiser, 1963).

The region under study contains many major upper crustal structural features (Fig. B1) whose origins are not clearly understood. It has been proposed that during the late Precambrian, an extensive series of geologic events occurred in the Midcontinent (Snyder, 1968). First,long periods of igneous activity over the entire Midcontinent resulted in the formation of the Keweenawan basin. This was followed by more igneous activity and the development of a major lineament (Midcontinent Geophysical Anomaly) dividing the Midcontinent. Subsidence, uplift, and erosion continued throughout the Paleozoic with the gradual formation of the basins and arches.

This sequence of events was, in part, responsible for the major structural features of the Precambrian basement distinguished by drill data (Cole, 1976). The Precambrian surface in northern Kansas is composed of a wide variety of igneous and metamorphic rocks, primarily of granitic affinity, except near the center of the Midcontinent Geophysical Anomaly (MGA) as discussed below (Bickford et al., 1979).

The Midcontinent Geophysical Anomaly (MGA) is the major Precambrian-aged feature from a geophysical viewpoint in the Central Stable Region (CSR). We prefer the MGA terminology as opposed to the equivalent Central North American Rift System (CNARS) or Midcontinent Rift because the name MGA is descriptive and not interpretive. The MGA extends laterally from Lake Superior (where the rocks that cause it crop out) through Kansas and possibly into Oklahoma (Yarger, 1983). It represents a 60-mgal gravity high flanked by 100-mgal gravity lows dissected in several places by possible transform faults (Chase and Gilmer, 1973). In Kansas, the MGA is a structure with suggested upper-mantle presence in the form of low P-wave velocity (Hahn, 1980). The magnetic influence of the MGA is seen quite clearly as highs of nearly 1000 gammas and flanking lows of several hundred gammas (Yarger,1983). A potential-fields model of the MGA by Yarger (1983) correlates a high density and highly magnetic rock body with bottom-hole basalt samples from the central part of the MGA (Bickford et al., 1979).

The Nemaha Ridge is another of the major structural discontinuities in the study area. Seismic reflection evidence suggests major uplift during late Mississippian time which produced the Nemaha ridge, forming the boundary between the Salina and Forest City basins in Kansas(Steeples, 1982). Aside from the MGA and Nemaha ridge, the Ozark uplift, Sioux uplift, Central Kansas uplift, Forest City basin, Anadarko basin, Denver basin, and Salina basin are structural features having some acoustical significance to this study.

Recent investigation of deep crustal structure in the study area was undertaken by the Consortium for Continental Reflection Profiling (COCORP) in 1979 with preliminary interpretation done by Brown et al. (1983). The seismic lines were chosen in order to sample subsurface points related to significant geophysical or geological features in Kansas. The structural features of particular interest to the investigators were the Nemaha ridge, the MGA, and the Humboldt fault. Deep crustal structure also was a primary target of the study.

The COCORP investigation in 1979 suggests the structure below 12 km is characterized by discontinuous, heterogeneous dipping layers with varying thicknesses (Serpa et al., 1984; Brown et al., 1983). In the small area being studied by COCORP, deep-reflection techniques show regions with possible large granitic intrusions and acoustically transparent zones. Below these granitic intrusions are acoustically significant layers with complex reflection patterns, many of which are assumed to be from outside the plane of the survey. The granitic-to-gabbroicrock inter-face may be of sufficient acoustic impedence contrast to cause the relative high reflectivity observed throughout this zone of apparent complex structure.

The COCORP investigation in Kansas has been unable to show a vivid continuous reflector from the 11-13 sec (34-38 km) zone which is the expected arrival time for the crust/mantle interface (Moho) throughout the survey area in Kansas. However, the character of energy returning from below the assumed Moho reflector zone has subtle irregularities and trace-appearance differences. The assumption is that these character changes are in some way related to the Moho (Serpa et al., 1984).

REVERSED REFRACTION STUDIES

The U.S. Geological Survey (USGS) shot reversed seismic-refraction profiles between Agate, Colorado, and Concordia, Kansas, in 1965 (Fig.B3). This section of the paper reports the authors' interpretation of the record sections from those profiles. The uninterpreted record sections are shown by Warren (1975). The USGS seismic refraction recording system is described by Warrick et al. (1961), and field procedures are outlined by Jackson et al. (1963).

Several refraction surveys have been performed previously in central North America. Jackson et al. (1963) calculated crustal thickness of 48 km and upper-mantle P-wave velocity of about 8.0 km/sec for an unreversed profile from eastern Colorado to southwestern Nebraska.Stewart and Pakiser (1962) calculated a crustal thickness of 51 km in eastern New Mexico from an unreversed profile obtained from the Gnome explosion. Tryggvason and Qualls (1967) determined a crustal thickness of 51 km and an upper mantle-velocity of 8.32 km/sec for a reversed northeast-southwest refraction profile centered near Oklahoma City.Stewart (1968) calculated an upper-mantle P-wave velocity of 8.0 km/sec a crustal thickness of 40 km for a reversed east-west profile in northern Missouri.

Little work has previously been done in Kansas on either crustal thickness or deep-crustal and upper-mantle velocities. Ewing and Press (1959) estimated the crust to be 35 km to 41 km thick from phase velocity of Rayleigh waves. Steinhart and Woollard (1961) estimated from gravity data and the assumption of isostasy at 96 km that the crust thickens to about 48 km at the west end from about 39 km at the east end of the present profile. Herrin and Taggart (1962) showed a P_n velocity of 8.1 km/sec to 8.3 km/sec, with the higher velocity occurring near the east end of the present profile.

Data

Shot information is reproduced from Warren (1975) in Table B1. Figs. B4-B6 show typical records reduced for a velocity of 6.0 km/sec. Reduced simply means that a rotation of the distance-versus-time coordinate system was made such that waves with a velocity of 6.0 km/sec arrive parallel to the distance axis. This allows quick analysis of the data and allows more data to be plotted in a small space. Note that the first arrivals have a velocity of approximately 6 km/sec out to a distance of about 180 km. Fig. B5 shows that close-in arrivals indicate at least two different sedimentary velocities above the 6-km/sec layer. Fig. B6 shows arrivals beyond 200 km that have phase velocities in excess of 8.0 km/sec. The linear least-squares fits of lines to the first arrivals beyond 200 km are:

<u>Eastward</u>	<u>Westward</u>
$T = 10.59 + \frac{X}{8.43}$	$T = 8.25 + \frac{X}{8.16}$

Interpretation

The following assumptions are made in the interpretation:

1) The distinct seismic velocities are associated with gently dipping layers separated by discontinuities.

2) The layer(s) beneath the granitic (5.99-6.15 km/sec) material are laterally homogeneous.

3) The measured first arrivals are the true first arrivals.

4) The compressional-wave velocities increase with depth.

Several of the record sections show two distinct arrivals out to a distance of about 15 km. The earlier set of arrivals commonly exhibits a velocity of 3.0 to 3.9 km/sec and are here interpreted to represent the arrivals through the Ogallala Formation, a Tertiary molasse deposit. The second set of arrivals has a phase velocity of 4.4 to 4.5 km/sec and is considered to be refracted arrivals with the velocity of the Paleozoic sediments except on the Stockton profile. The 4.45-km/sec arrival is first and direct at Stockton because the Ogallala Formation has been eroded away at the shot point.

The thickness calculated for the sediments in Colorado (Hale East)is 2.6 km compared to a known thickness of 2.5 km from drill evidence. At Stockton the sedimentary thickness is calculated to be 2.0 km compared to a known sedimentary thickness of 1.3 km. The discrepancy is due to an increase in sedimentary thickness westward from the Stockton shotpoint to the recording sites and because the Ogallala Formation is present at the recording sites but absent at the shot point. These two effects cause a larger intercept time and, hence, an erroneously large calculated sedimentary thickness.

The arrivals commonly assigned to granites (5.9-6.15 km/sec) arrive first from a distance of about 5-6 km to a distance of more than 180 km(see Figs. B6a and B6b). A somewhat gradual increase in the velocity of the granitic layer seems to occur with depth, so a single least-squares line was fit to the data providing an average velocity. The thickness of the granitic layer is highly dependent upon whether the interpretation includes a deeper mafic (6.7-7.2 km/sec) layer. The evidence for this layer is not overwhelming or necessarily unique, though it has been used by most investigators in the Midcontinent (Stewart, 1968; Tryggvason and Qualls, 1967; Jackson, et al., 1963). While clear evidence of these intermediate crustal velocities exists, clear evidence for a continuous layer or layers does not. COCORP studies in the northeastern part of Kansas suggest these higher velocities are caused by mafic plutons intruded into the lower crust (Brown et al., 1983; Serpa et al., 1984). If interpretation is done using a deep crustal layer of 6.7 to 7.2-km/sec velocity, the effect is to make the crust seem about 5 km thicker.

Some evidence of a Moho reflection on Fig. B6b is found at a distance of 130 to 155 km. This event, if it is a reflection, suggests an average crustal velocity of 6.2 km/sec. This interpretation implies a Moho depth of 40 km near the middle of the refraction line.

Fig. B6c shows the P-arrival data from a distance of 230 km to 410 km westward from the Concordia shot point. The least-squares fit of 8.16 km/sec is shown on the figure to highlight the first arrivals. Fig. B6d similarly displays the data from 220 km to 430 km eastward from the Agate shotpoint, with the first arrival phase-velocity of 8.43 km/sec highlighted.

Discussion

Fig. B7 shows a cross sectional model of the refraction data. The resulting crustal thickness in eastern Colorado (46 km) is a couple of kilometers thinner than previously calculated for an unreversed profile by Jackson et al. (1963). The calculation of a 36-km thick crust in north-central Kansas at the west edge of the MGA is thinner than might have been expected on the basis of previously mentioned results in Missouri and Oklahoma. This number is reasonable, however, as discussed later.

The P_n velocity at the top of the upper mantle is high enough that it deserves special attention. The phase velocities of P_n are 8.16 km/sec for the westward direction and 8.43 km/sec for the eastward direction. This in itself shows that the crust must thicken to the west. When the problem is solved for the general dipping case, a true P_n velocity of 8.29 results while the dip angle is 1.03° westward for the crust-mantle interface measured from the topographic surface. This high velocity is not caused by picking errors on the seismograms, since such errors usually involve late picks, resulting in lower apparent velocities.

The P_n velocity reported here is nearly equal to the highest P_n velocity reported in the United States (8.32 km/sec in Oklahoma by Tryggvason and Qualls, 1967) and the 8.43 km/sec P_n phase velocity for the eastward profile is the highest reported. Some investigators have shown P_n phase velocities in excess of 8.4 km/sec at distances exceeding 445 km in Canada (Mereu and Hunter, 1968; Eisler and Westphal, 1967),but data in the present work are not recorded beyond about 440 km.

GRAVITY DATA

Fig. B8 shows regional gravity data excerpted from a USGS gravity map of the United States. Note the regional gravity increases steadily eastward. The gradient is almost exactly parallel to the seismic profile of this study which is one reason the line was shot at this location with the east-west orientation. A least-squares fit of a linear gradient to the observed gravity contours along the seismic profile shows the Bouguer anomaly to increase rather uniformly eastward by 0.27 mgal/km. Thus a direct comparison of the gravity model and the seismic data is relatively simple.

The gravity modeling was done using the approximation presented by Nettleton (1976, p. 201-203) as follows

$$\Delta g = 41.93 \, LT \tan \theta \qquad (1)$$

where Δg is gravity difference in milligals, L is the distance in kilometers,θ is the dip angle between points A and B, and T is the density contrast between layers. For θ of about 11° this approximation introduces error of only 3%, so the errors arising here from the approximation should be less than 0.3% because θ is about 1° for the model discussed. Gravity fields may be calculated for individual dipping layers, then summed to produce the gravitational effects for each model.

Most of the observed 120-mgal change in the Bouguer anomaly must be due to deep structure, as only about 6 mgal could be due to changes within the sedimentary cover (Woollard, 1959). As mentioned earlier, Steinhart and Woollard (1961) assumed isostatic compensation at 96 km depth to estimate crustal thinning of 10 km along this seismic profile. On the basis of Bouguer anomalies, they estimated a crustal thickness of 48 km at the west end and 39 km at the east end of the profile. That estimate is consistent with the combined gravity and seismic-refraction results from the present study, although our comparable numbers are 46 km and 36 km, respectively. The density contrast between the crust and upper mantle needed to satisfy the 10 km of crustal thinning is 0.32 gm/cm^3. This is a reasonable number--possibly a bit lower than might be expected.

REGIONAL-EARTHQUAKE TRAVEL TIMES

In the previous section of this paper, reversed-refraction profiles with a maximum source separation of 500 km (Concordia, Kansas, to Agate, Colorado) were used to develop crustal models for western Kansas. In this section of the paper analysis of compressional wave arrivals from regional (epicentral distance greater than 250 km) earthquake seismograms is used to study the crust and upper mantle in eastern Kansas.

The use of earthquakes as the energy source for refraction profiles has not been extensively investigated. Developing a crustal model for use in earthquake-location routines from earthquake refraction analysis eliminates the inherent error of explosion-derived model resulting from the dissimilar nature and location of the source. Earthquakes in the Midcontinent typically occur several kilometers beneath the earth's surface, whereas explosive sources necessarily occur very near the surface. Much of the travel-time variation from regional distances can occur within the upper few kilometers of the crust.

Receiver Network

The earthquake network in Kansas began operation at a high level of sensitivity in December 1978. The nine-station network was designed and installed to locate microearthquakes along potentially active geologic features in eastern and central Kansas (Fig. B9). The network possesses the sensitivity necessary to locate events with duration magnitude as low as 1.5 in the eastern half of Kansas (Sheehan and Steeples, 1983). Funding for the stations was provided by the United States Nuclear Regulatory Commission (NRC) and the Kansas City District, U.S. Army Corps of Engineers.

Residuals

As a head wave propagates across the network, it interacts with anomalous velocity zones that originate and/or terminate within the network. If heterogeneities of this sort exist, energy propagation across the network will be nonlinear in time. The size of the time variation (Δt) is dependent on the size and orientation of the anomalous (Δt) zone and the velocity contrast between zones (V_2, V_1).

$$\Delta t = \frac{\Delta h\,(V_2 - V_1)}{(V_2 * V_1)}. \quad (2)$$

P_n arrivals, by definition, penetrate all layers of the crust. Any major anomalous zone between the crust/mantle interface and the ground surface (within a volume defined by the areal extent of the network and the critical angle of the crust/mantle interface) should result in a deviation in the actual from the expected arrival time of a head wave through a homogeneous medium. The residual values are directly related to the deviation in actual arrival time from expected.

The calculation of residuals is implemented with one assumption.The least-squares determined slope of the line intersecting the first-break times at the proper source/receiver offset is the true apparent velocity for the layers. Then with the use of the equation for a line,residuals are calculated by the following equation:

$$\text{Residual} = \text{Arrival Time} - \frac{\text{Epidistance - Y Intercept}}{\text{Velocity}} . \qquad (3)$$

From the travel-time residuals (i.e., the amount of time a phase arrival deviates from the straight-line approximation of the apparent velocity of propagation), a characteristic directional delay or early arrival for each station can be identified. Certain stations show consistently late or early arrivals, depending on crust and upper-mantle anomalies. Using a statistical approach of determining directional delays enables interpretation of velocity anomalies and apparent unconformities within the subsurface of the sampled area.

Data Analysis

Picks of impulsive first-break energy (P_n) inherently carry more integrity than picks of energy arrivals later in the wave train (Pakiser and Steinhart, 1964). Therefore, all analysis of earthquake energy on seismograms will be restricted to the first arrivals. Events chosen for this study had sufficient energy to arrive at a majority of the receiver stations as an impulsive first arrival. For most stations, this would amount to an instantaneous change in amplitude of approximately 20 dB. Events 8, 9, 10, 11, and 12 were located by the Oklahoma Geophysical Observatory and have general progression patterns from south-southwest into the network with epicentral distances ranging from 365 km for the closest station to about 900 km for the most distant station with discernible phase arrivals. The 5 south events are plotted with a vertical tick indicating time and amplitude of each interpreted phase arrival (Fig. B10). Events 8 and 9, originating within Oklahoma, show very similar wave-train character (Fig. B11). An apparent velocity of 8.35 km/sec 0.15 km/sec for the crust/mantle interface recorded by these two events is within the experimental error of previously obtained values (Tryggvason and Qualls, 1967). Events 10, 11, and 12 originated from the Texas Panhandle region. Event B12 has features that closely resembled the two Oklahoma events (8 and 9). The slight variation in values might be associated with subtle regional changes in crustal thickness and upper crustal heterogeneities. Comparison of events 8, 9,and 12 gives a model with a large subsurface sampling area. This model,however, would not show the proposed Moho low in central Oklahoma (Warren and Healy, 1973).

The upper crustal structure between the eastern events and the recording network is very complex (Stewart, 1968). Events 2, 3, and 4 were used as indicative of the subsurface to the east (Fig. B12). These events show good P_n velocity agreement within themselves, with an average of 8.21 km/sec ±0.15 km/sec. They also all have epicenters in the Mississippi Embayment. Earthquakes that originate from outside a concentrated grouping in northeastern Arkansas lack regional consistency and are used predominantly for station residual determinations.

Event 6, originating in Kentucky, contained sufficient energy to saturate the analog recorders. All significant information beyond excellent first-break energy was clipped. Event 6 has an epicentral distance greater than any other studied here. After rejection of LAK and EDK from the data set due to poor correlation to the least-squares line, an apparent P_n velocity of 8.87 km/sec ±0.15 km/sec, was obtained at offsets from about 1,000 to 1860 km from the source. This observation is discussed in more detail later in this paper.

Events 13, 14, and 15 are the northern data set (Fig. B13). These three events have calculated epicenters with horizontal separation between events 13 and 15 of approximately 580 km and between events 13 and 14 of 150 km. Event 15 has an emergent P_n arrival and was therefore not used to determine the P_n velocity from the north. Events 13 and 14 have apparent Pn velocities that show good consistency, very little deviation, and were calculated from picks of impulsive first breaks.For those reasons the apparent P_n velocity for the northern crust is formulated using events 13 and 14. The apparent P_n velocity from the north is 8.38 km/sec 0.15 km/sec.

As characteristic of many seismic-refraction surveys when applying statistical techniques, lack of sufficient data poses a sizeable difficulty in interpreting data on travel curves (Borcherdt and Healy, 1968). This problem was encountered in dealing with energy arrivals originating in the west. Only one event falls within the guidelines for data acceptance. From event 16, an apparent P_n velocity of 8.59 km/sec ±0.15 km/sec was calculated.

Discussion

Using earthquakes as the energy source for refraction surveys restricts much of the control over the data set that is present on conventional refraction profiles. Since the stations are concentrated in eastern Kansas in a somewhat circular array (Fig. B9), refraction-type studies, using the stations as receivers, lack the two-dimensional precision of conventional refraction studies. However, by using a great circle technique of station alignment, regional features should have only minor distortion (assuming proper sampling). Thus, by comparing several good-quality events arriving at the network from the same general direction, certain acoustic properties and apparent structural anomalies of the crust and upper mantle can be identified.

An anomalous high-velocity crust in the northwestern portion of the network can be interpreted from P_n residuals (Fig. B14). The presence of such a velocity anomaly has been suggested in previous studies (Lui,1980; Serpa et al., 1984). Good correlation can be found between the potential fields model and the seismic-velocity delay model (Yarger,1983). Transition of a P-wave from a granitic crust, which is commonly accepted as the predominant crustal rock type in the area, into a basaltic environment could give velocity residuals similar to those observed here. The size of the residual, of course, also is dependent upon height of the anomalous rock column. Exact determination of the anomalous body's boundaries using the existing station array is not possible. Boundaries can be estimated using the stations within the anomalous material as control points for a minimum affected area. In general, the anomalous high-velocity area includes CNK, SNK, MLK, and TCK (Fig. B14). Also, localized patches of anomalous crust are found in the central part of the station array many times only observed on one or two stations.

Consistently-late arrivals at EDK from regional events could be related to a geophysical anomaly previously detected and its borders defined by an aeromagnetic study of Kansas (Yarger, 1983). The anomaly is represented by a low of 600 gammas centered near EDK. A continental collision zone has been given as a possible explanation for the low (Yarger, 1983). Rock types at the Precambrian surface in the area lack any evidence for the presence of this aeromagnetic low (Bickford et al.,1979). However, some type of plate-convergence process, which could have been operational during mid-Proterozoic time, has been suggested (Van Schmus and Bickford, 1983). Local-event residuals do not suggest the presence of low-velocity material in the upper part of the crust. The arrival-time patterns observed are therefore consistent with both the shallow Precambrian geology of Bickford et al. (1979) and Van Schmus and Bickford, (1983) and the hypothesized collision zone of Yarger (1983).

Examination of first-arrival P-wave residuals from event 6 (from Kentucky) reveals possible evidence for a low-velocity upper mantle near the MGA. An apparent P-wave velocity of 8.87 km/sec 0.15 km/sec was calculated for a 1,000 km to 1,860 km source-to-receiver offset. Previous studies in the Midcontinent have documented a 328-km-deep velocity discontinuity with a 9.27 km/sec 0.05 km/sec velocity at a source/receiver offset of 1700 km (Masse, 1973). Assuming the documented velocity is representative of the

Midcontinent at the indicated offsets, the slower velocity observed here at similar offsets could be the result of a low-velocity upper mantle beneath the network. The observed velocity and suggestion of a lower-velocity upper mantle is consistent with observations and conclusions drawn from teleseismic P-wave arrivals by Hahn, (1980). Only event 6 had sufficient source/receiver offset for the first arrivals to be refractions from a sub-Moho velocity discontinuity.

Within the crust, complex reflection patterns from COCORP data have been hypothesized to be the result of either gneissic banding, interlayering of granite and restites relating to anatexis or mafic intrusions (Serpa et al., 1984). Complex structure results in multiple interactions with anomalous velocity zones, complicating the interpretation. Refracted waves originating from within this complicated structure would lack good continuity and arrival consistency from one surface location to the next. Therefore, interpretation of intermediate layer depths and velocities from secondary compressional-wave phase arrivals is speculative at best. This applies to both the reversed-refraction data and the earthquake-arrival data.

Exact determination of a crustal model using the earthquake data set has not proven to be totally successful. However, from analysis of P_n energy incident on the network from different directions, specific characteristics of the crust and upper mantle can be identified. Certain characteristics (amplitude of intermediate arrivals, frequency of impulsive head waves, etc.) of the P-wave arrivals studied showed dependence on local geology and direction from which the energy originated. Assuming gross consistency in characteristic velocities, approximate trends in layer dip and directional-station delays can be determined. From the four apparent P_n-wave velocities determined for each direction data set, the Moho dips away from the study area to the west, north, and south, and seems to level off to the east. The velocity of the upper mantle is approximately 8.25 km/sec ±0.15. Station delays could indicate anomalous velocity zones or crustal heterogeneities possibly representative of previous tectonic activity or vulcanism.

CONCLUSION

Reversed-refraction profiles show that the crust-mantle interface has an apparent dip of 1 westward along the profile in Fig. B3. The linear-gravity gradient shown in Fig. 6 is virtually parallel to the refraction profile, suggesting that the 1 dip value is probably true dip. Crustal thinning of the order of 10 km occurs between eastern Colorado and north-central Kansas. Density contrast of 0.32 gm/cm^3 at the Moho simultaneously fits the gravity data and the seismic refraction data.

Earthquake P_n-wave residuals were used to postulate the presence of several anomalous velocity areas (Fig. B14). Earthquake stations CNK,BEK, TCK, and MLK clearly define an anomalous zone in the crust with a high-velocity center flanked by low-velocity borders on the east and west (high and low velocities are qualitative with respect to the average crustal velocities over the entire network). This strengthens the results of Lui (1980) and Serpa et al. (1984) that a high-velocity crust exists beneath the MGA. Consistent delays in the P_n wave at EDK may result from the same anomalous zone that causes a strong aeromagnetic low centered near EDK previously identified by Yarger (1983).

REFERENCES

Bickford, M. E., Harrower, K. L., Nusbaum, R. L. Thomas, J. J., and Nelson, G. E., 1979, Preliminary geologic map of the Precambrian basement rocks of Kansas: Kansas Geological Survey, Map M-9, Scale 1:500,000.

Brookins, D.G., and Meyer, H.O.A., 1974, Crustal and upper mantle stratigraphy beneath eastern Kansas: Geophys. Res. Letters, v. 1, no. 6, p. 269-272.

Borcherdt, R.D., and Healy, J.H., 1968, A method for estimating the uncertainty of seismic velocities measured by refraction techniques: Seism. Soc. Am. Bull., v. 58, no. 6, p. 1,769-1.790.

Brown, L., Serpa, L., Setzer, T., Oliver, J., Kaufman, S., Lillie, R., Steiner, D., and Steeples, D., 1983, Intra-crustal complexity in the U.S. Midcontinent: Preliminary results from COCORP surveys in N.E. Kansas: Geology, v. 11, p. 25-30.

Chase, C., and Gilmer, T., 1973, Precambrian plate tectonics: The Midcontinent gravity high: Earth and Planetary Sci. Let., v. 21, p. 70-78.

Cole, V. B., 1976, Configuration of the top of the Precambrian rocks in Kansas: Kansas Geological Survey Map M-7, scale 1:500,000.

Eisler J. D., and Westphal, W. H., 1967, Lake Superior seismic experiment--Ontario-Quebec refraction profiles: Stanford Res. Inst. Final Sci. Rept. to AFOSR, 33 p.

Ewing, W. M., and Press, F., 1959, Determination of crustal structure from phase velocity of Rayleigh waves, 3--the United States: Bull, Geo. Soc. Am., v. 70, no. 3, p. 229-244.

Hahn, R. K., 1980, Upper mantle velocity structure in eastern Kansas from teleseismic P-wave residuals: M.S. thesis, University of Kansas, Lawrence, KS, p. 85.

Hahn, R. K., and Steeples, D. W., 1980, Upper-mantle velocity structure in eastern Kansas from teleseismic P-residuals (abs.): EOS Trans. Amer. Geophys. Union, v. 61, p. 1,046.

Herrin, E., and Taggart, J., 1962, Regional variations in P_n velocity and their effect on the location of epicenters: Seism. Soc. Am. Bull., v. 52, no. 5, p. 1,037-1,046.

Jackson, W. H., Stewart, S. W., and Pakiser, L.C., 1963, Crustal structure in eastern Colorado from seismic refraction measurements: J. Geophys. Res., v. 68, p. 5,767-5,776.

Lui, C. Y., 1980, Microearthquake in Red Willow County, Nebraska: M. S. thesis, University of Kansas, Lawrence, p. 53.

Masse, R. P., 1973, Compressional velocity distribution beneath central and eastern North America: Seism. Soc. Am. Bull., v. 63, no. 3, p. 911-935.

Mereu, R. F., and Hunter, J. A., 1968, Crustal and upper mantle structure under the Canadian shield from Project Early Rise data: Seismo. Soc. Am. Bull., v. 59, p. 147.

Miller, R. D., 1983, Crustal study in Kansas using earthquake seismograms: M.S. Thesis, University of Kansas, Lawrence, 105 p.

Nettleton, L.L., 1976, Gravity and magnetics in oil prospecting: McGraw-Hill, 464 p.

Pakiser, L.C., 1963, Structure of the crust and upper mantle in the western United States: J. Geophys. Res., v. 68, no. 20, p. 5,747- 5,756.

Pakiser, L.C., and Steinhart, J.S., 1964, Explosion seismology in the western hemisphere; Research in Geophysics, v. 2: Solid earth and interface phenomena, Mass. Inst. of Tech. Publ. p. 123-147.

Pakiser, L.C., and Zietz, I., 1965, Transcontinental crust and upper-mantle structure: Reviews of Geophysics, v. 3, no. 4, p. 505-520.

Serpa, L., Setzer, T., Farmer, H., Brown, L., Oliver, J., Kaufman, S., Sharp, J., and Steeples, D. W., 1984, Structure of the southern Keweenawan rift from COCORP surveys across the Midcontinent Geophysical Anomaly in northeastern Kansas: Tectonics, v. 3, p. 367-384.

Sheehan, A., and Steeples, D.W., 1983, Sensitivity of Kansas microearthquake network: Earth Notes, v. 54, no. 2, p. 13-21.

Snyder, F. G., 1968, Tectonic history of midcontinental United States: UMR Journal, no. 1, p. 65-77.

Steeples, D. W., 1976, Preliminary crustal model for northwest Kansas (Abs.): EOS, Trans. AGU, v. 57, p. 961.

Steeples, D. W., 1982, Structure of the Salina-Forest City interbasin boundary from seismic studies: Univ. of Missouri-Rolla Jour. no. 3, p. 55-81.

Steinhart J. S., and Wollard, G.P., 1961, Seismic evidence concerning continental structure; in Explosion studies of continental structure, Editors J.S. Steinhart and R.P. Meyers: Carnegie Inst., Wash. Publ. 622, p. 344-383.

Stewart, S. W., 1968, Crustal structure in Missouri by seismic refraction methods: Seismol. Soc. Am. Bull., v. 58, p. 291-293.

Stewart, S. W., and Pakiser, L. C., 1962, Crustal structure in eastern New Mexico interpreted from the Gnome explosion: Seismol. Soc. Am. Bull. v. 52, p. 1,017-1,030.

Tryggvason, E., and Qualls, B. R., 1967, Seismic refraction measurements of crustal structure in Oklahoma: J. Geophys. Res., v. 72, p. 3,738-3,740.

Van Schmus, W. R., and Bickford, M. E., Proterozoic chronology and evolution of the midcontinental region, North America; in Precambrian Plate Tectonics, by A. Kroner, editor: Elsevier, NY, in press.

Warren, D.H., and Healy, J.H., 1973, Structure of the crust in the conterminous United States: Tectonophysics, v. 20, p. 203-213.

Warren, D. H., 1975, Record sections for the seismic refraction profile Agate-Concordia, eastern Colorado and western Kansas: U.S. Open-file Report 75-380, p. 46.

Warrick, R. E., Hoover, D. B., Jackson, W. H., Pakiser, L. C., and Roller, J. C., 1961, The specifications and testing of a seismic-refraction system for crustal studies: Geophysics, v. 26, p. 820-824.

Woollard, G. P., 1959, Crustal structure from gravity and seismic measurements: J. Geophys. Res., v. 64, p. 1,521-1,544.

Yarger, H. L., Ng, K., Robertson, R., and Woods, R., 1980, Bouguer gravity map of northeastern Kansas: Kansas Geological Survey, scale 1:500,000 map..

Yarger, H. L., 1983, Regional interpretation of Kansas aeromagnetic data: Kansas Geological Survey, Geophys. Series 1, 35 p.

TABLE CAPTIONS

Table B1. Shot information from Warren (1975).

TABLE B1

SHOT INFORMATION

Name and number	May 1965 date	Time, Mountain Daylight	Size, pounds	Latitude North	Longitude West
Agate 1	11	07:00:00.27	20,000	39°33.95'	103°44.86'
Hale 1	6	07:00:00.27	150	39°34.41'	102°07.31'
Hale 2	6	11:30:00.53	500		
Brewster 1	6	06:30:00.34	500	39°35.03'	101°25.61'
Brewster 2	6	12:00:00.36	150		
Brewster 3	7	07:00:00.35	150		
Brewster 4	7	11:30:00.35	500		
Brewster 5	9	20:50:00.16	1,000		
Brewster 6	10	07:20:00.30	1,500		
Brewster 7	10	12:00:00.29	2,500		
Brewster 8	10	17:00:00.31	4,000		
Selden 1	7	06:30:00.45	500	39°34.40'	100°41.90'
Selden 2	7	12:00:00.44	150		
Selden 3	9	20:00:00.34	150		
Selden 4	10	07:40:00.57	500		
Lenora 1	6	06:00:00.24	4,000	39°34.79'	100°04.45'
Lenora 2	6	11:00:00.09	2,500		
Lenora 3	7	06:00:01.04	1,500		
Lenora 4	7	11:00:01.09	1,000		
Lenora 5	9	20:30:00.41	500		
Lenora 6	10	08:00:00.36	150		
Lenora 7	10	12:40:00.41	150		
Lenora 8	10	17:20:00.34	500		
Stockton 1	10	12:20:00.46	510	39°34.97'	99°20.82'
Stockton 2	10	17:40:00.56	150		
Concordia 1	12	05:00:00.63	20,000	39°31.22'	97°54.67'

FIGURE CAPTIONS

Fig. B1. Major structural features within the study area as described by Snyder (1968).

Fig. B2. Paths of major compressional waves through the crust.

Fig. B3. Location of line of shots. Open circles show shot points; recordings were made along dashed line.

Fig. B4. A typical reduced record section (time vs. distance curve). The heavy dark line shows interpreted direct wave (sedimentary veneer) and first defraction.

Fig. B5. On the very near traces, two distinctly different sedimentary velocities can be interpreted.

Fig. B6. a) Arrivals to distances of 175 km shot westward from Lenora, Kansas.
b) Arrivals to distances of 180 km shot eastward from Brewster, Kansas.
c) The reduced time-distance curve here shows arrivals from receivers greater than 200 km westward away from the shot near Concordia, Kansas.
d) The reduced time-distance curve here shows arrivals from receivers greater than 200 km eastward from the shot near Agate, Colorado.

Fig. B7. Cross section showing crustal thickness average velocity of the crust, and velocity of the upper mantle. This cross section directly correlates to the regional gravity-gradient plot of Fig. 8.

Fig. B8. The regional gravity gradient was measured along the profile from Concordia, Kansas, to Agate, Colorado. The gravity data agree quite well with the reversed-refraction profile-derived cross section.

Fig. B9. Kansas Geological Survey's earthquake stations in conjunction with mapped faults (˚ = station locations; / = faults).

Fig. B10. All events from the south used in the formulation of the residual model.

Fig. B11. Events from the south used to determine correlation of phase.

Fig. B12. All events fromt he east used in the formulation of the residual model.

Fig. B13. All events fr

Fig. B14. P_n residuals interpretation.

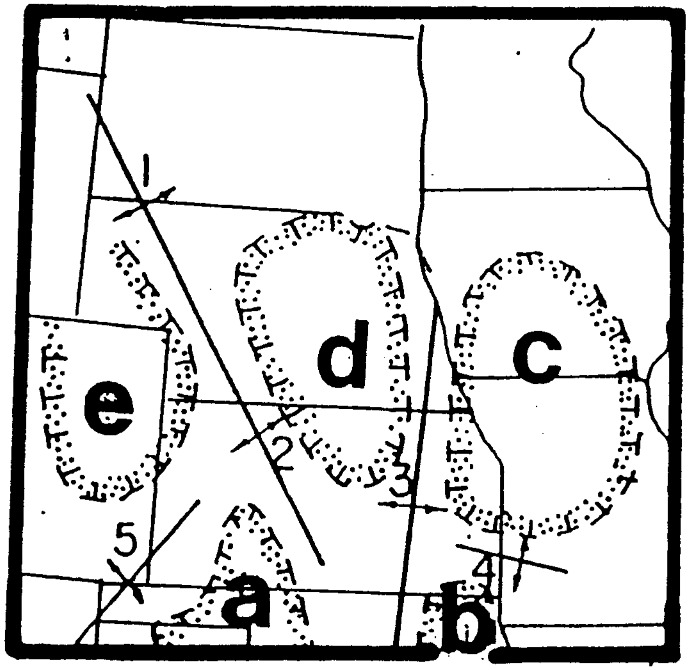

Uplifts

1. Cambridge
2. Central Kansas
3. Nemaha
4. Bourbon
5. Las Animas

Basins

a. Hugoton
b. Cherokee
c. Forest City
d. Salina
e. Denver

Figure B1.

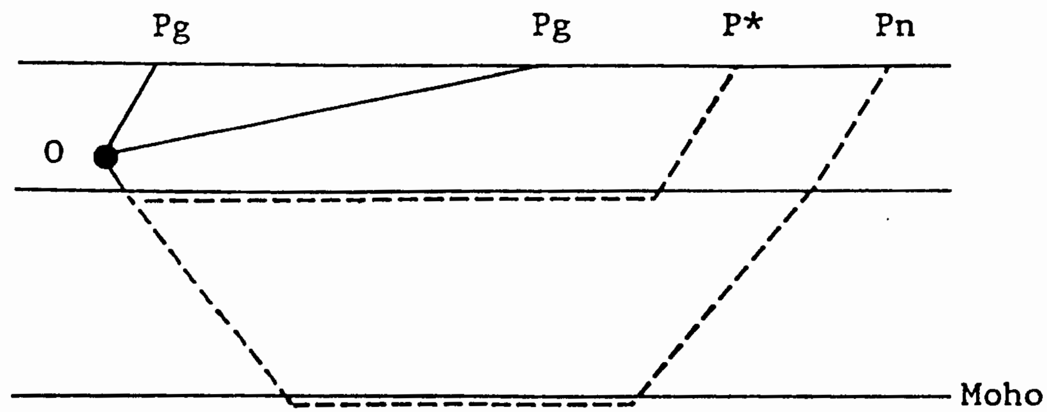

Figure B2.

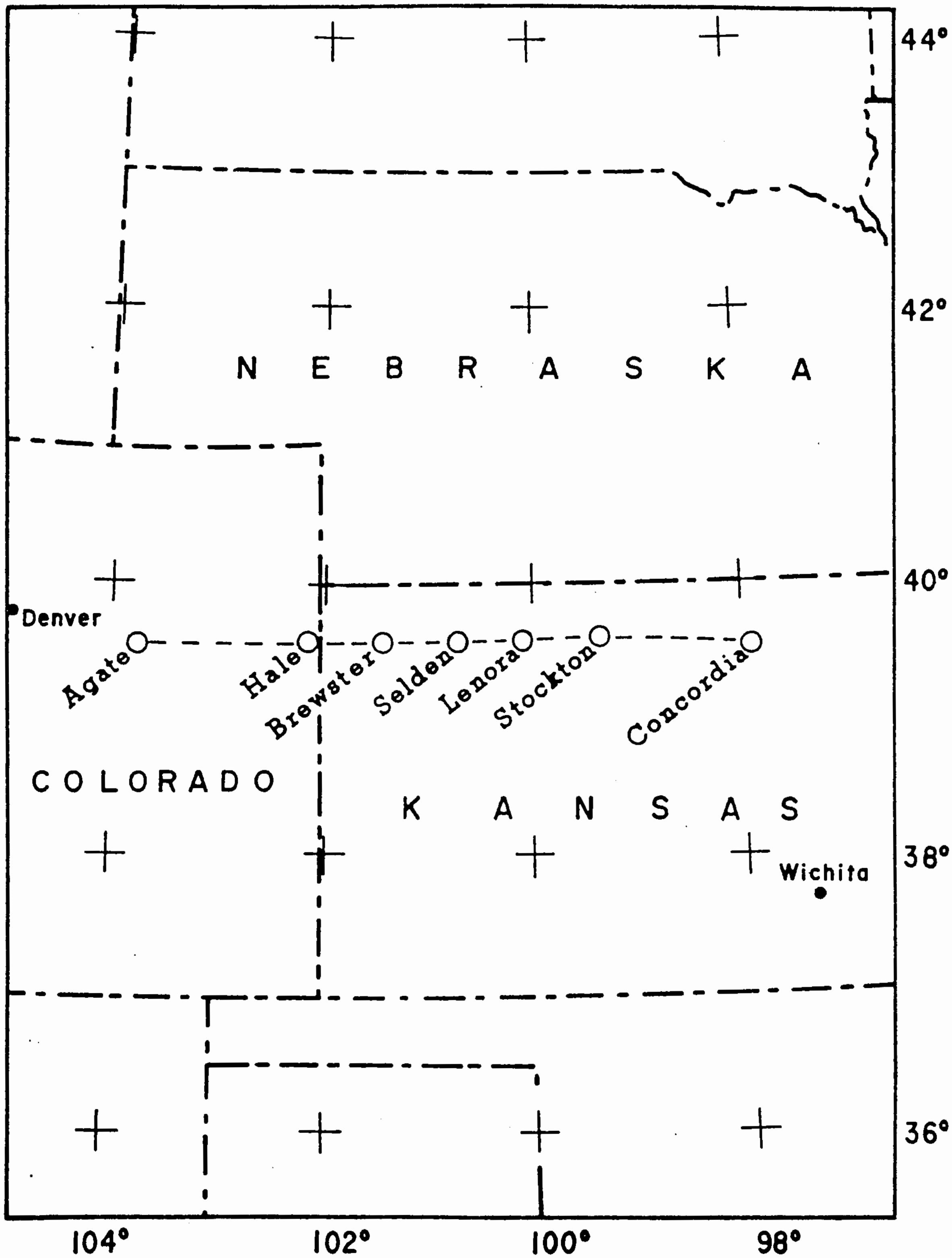

44°
42°
40°
38°
36°
104°
102°
100°
98°
N E B R A S K A
Denver
Agate
Hale
Brewster
Selden
Lenora
Stockton
Concordia
COLORADO
K A N S A S
Wichita

Figure B3.

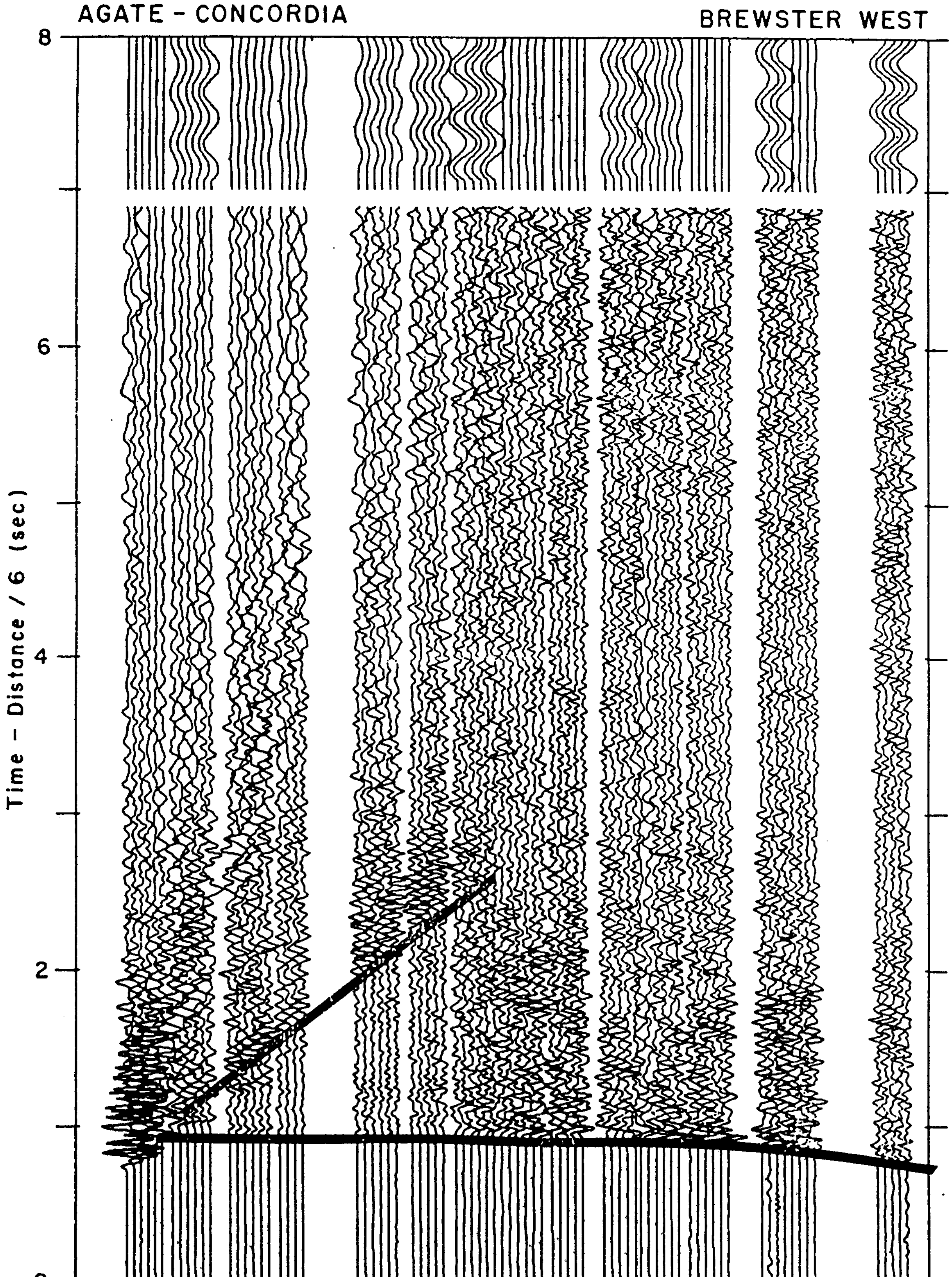
AGATE - CONCORDIA
BREWSTER WEST
Time - Distance / 6 (sec)
8
6
4
2
0
0
20
40
Distance (km)

Figure B4

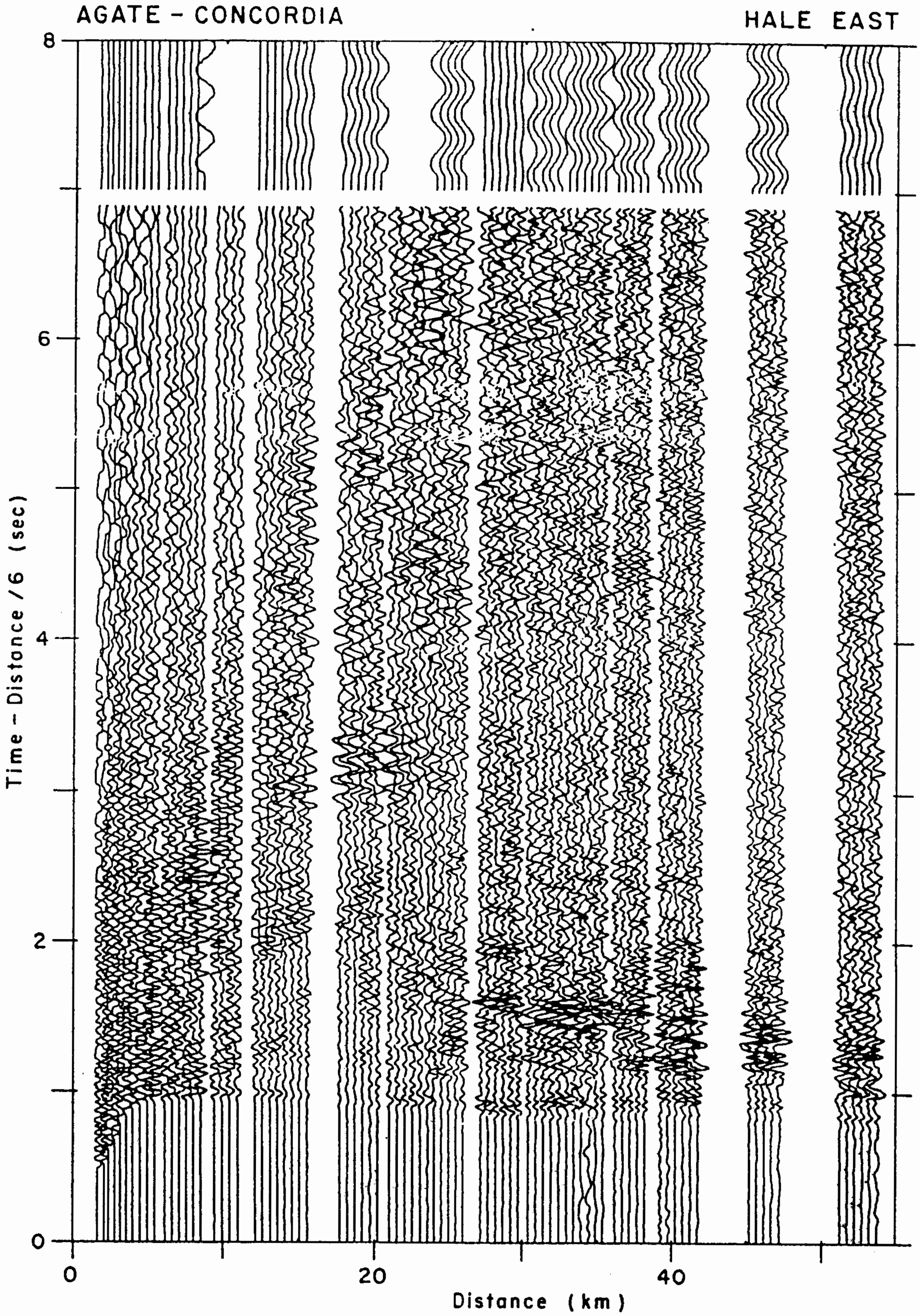
AGATE - CONCORDIA
HALE EAST
Time - Distance /6 (sec)
8
6
4
2
0
0
20
40
Distance (km)

Figure B5.

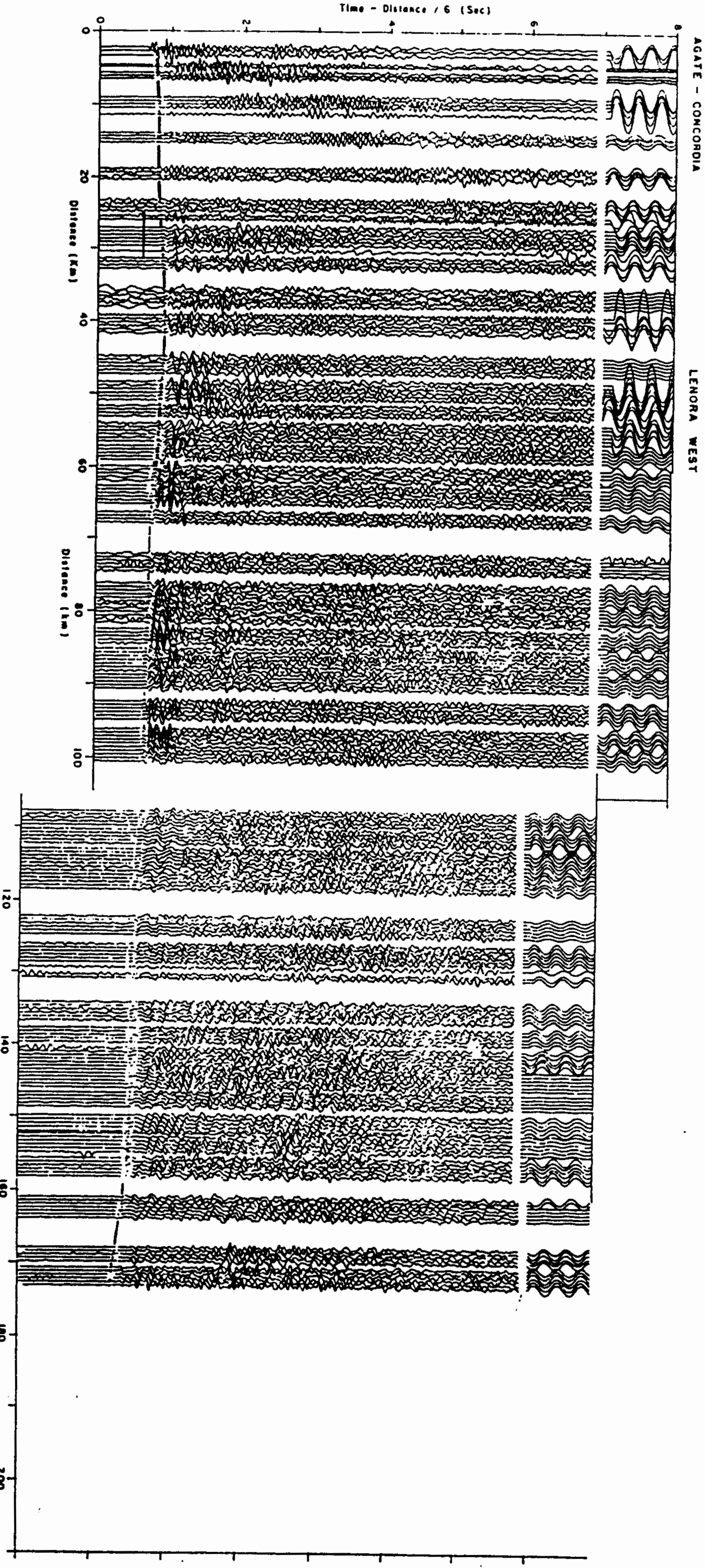
Time - Distance / 6 (Sec)
AGATE - CONCORDIA
LENORA WEST
Distance (Km)
Distance (km)
0
2
4
6
8
20
40
60
80
100
120
140
160
180
200

Figure B6a.

Figure 6b.

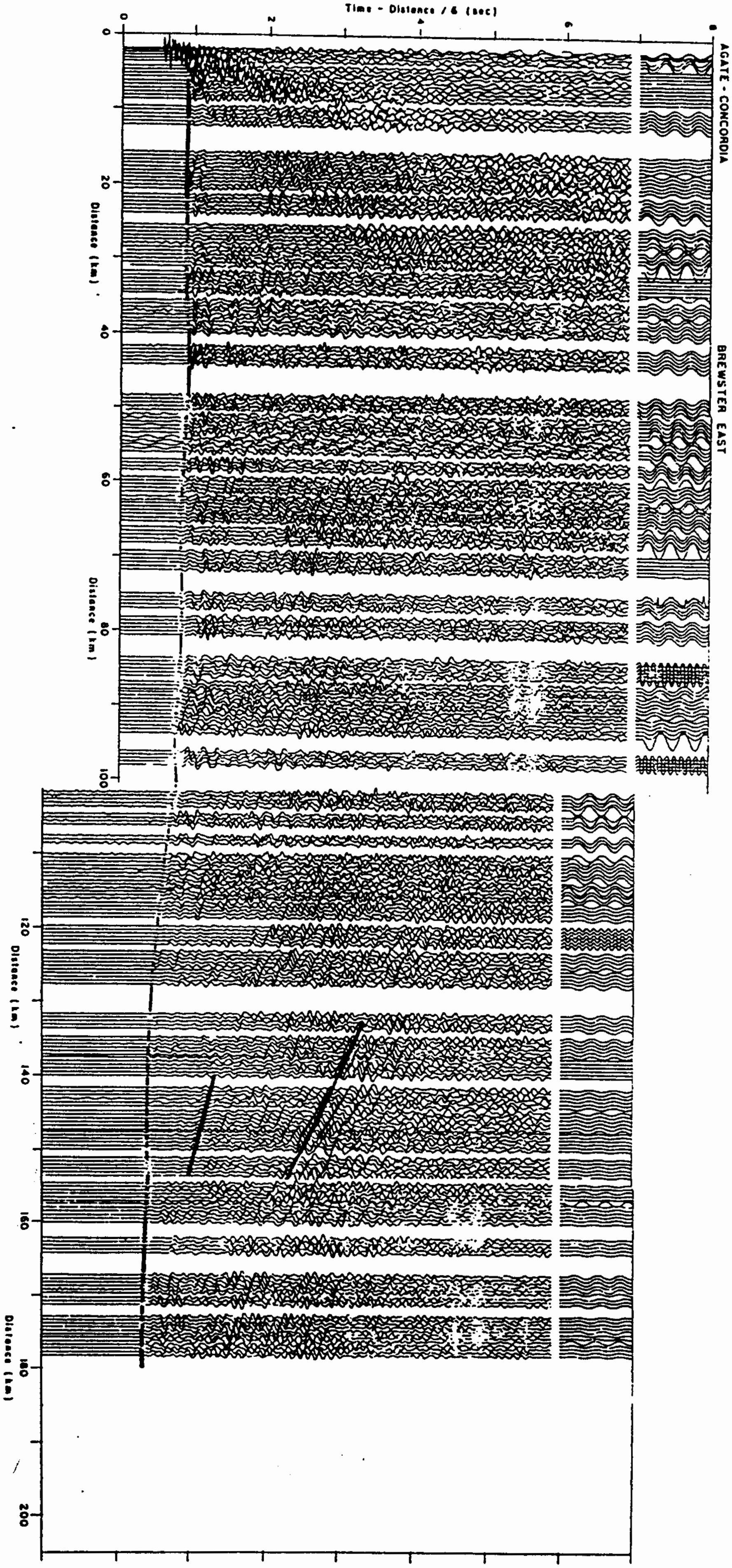
Time - Distance / 6 (sec)
AGATE - CONCORDIA
BREWSTER EAST
Distance (km)
Distance (km)
Distance (km)
Distance (km)

Figure 8oc

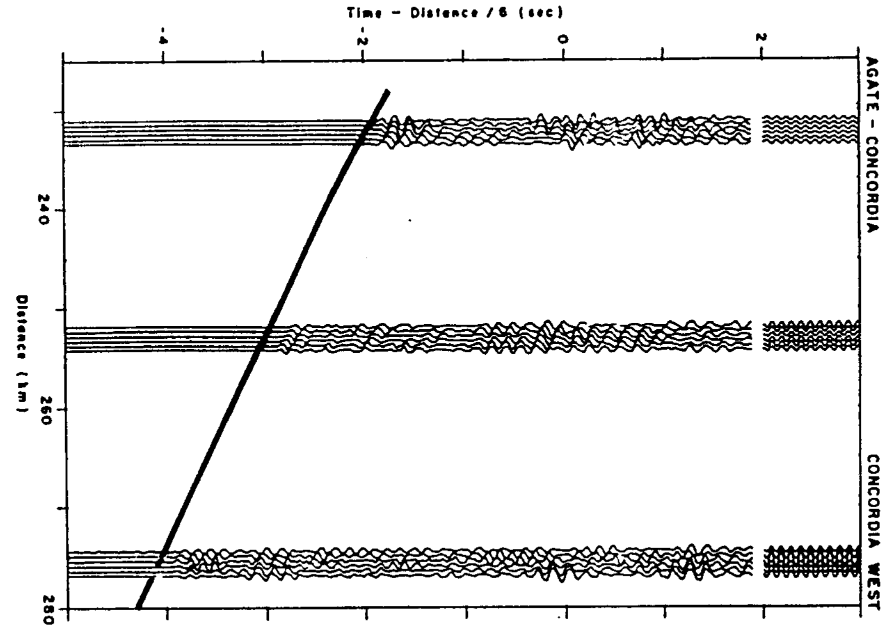
Time - Distance / 6 (sec)
-4
-2
0
2
AGATE - CONCORDIA
CONCORDIA WEST
240
260
280
Distance (km)

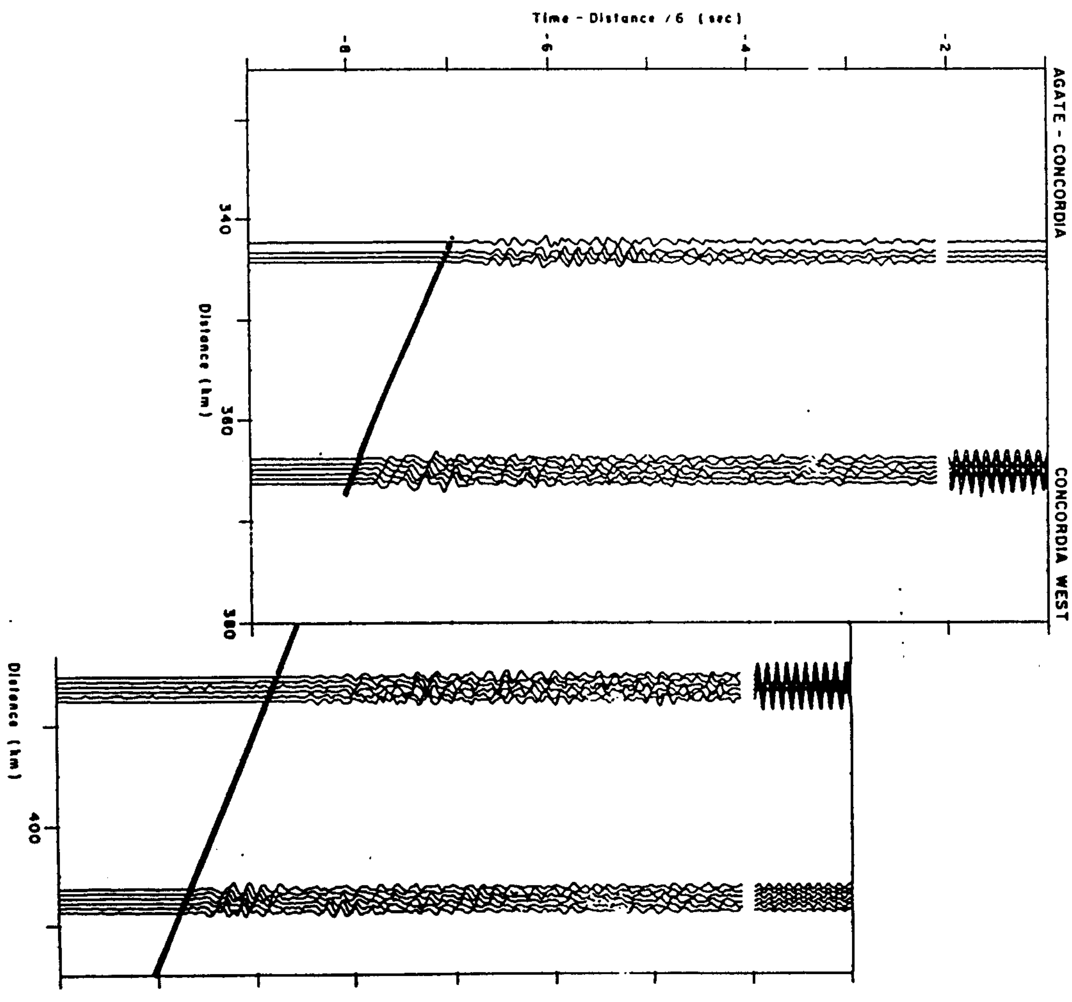
Time - Distance / 6 (sec)
-8
-6
-4
-2
AGATE - CONCORDIA
CONCORDIA WEST
340
360
380
400
Distance (km)

Figure 5bd.

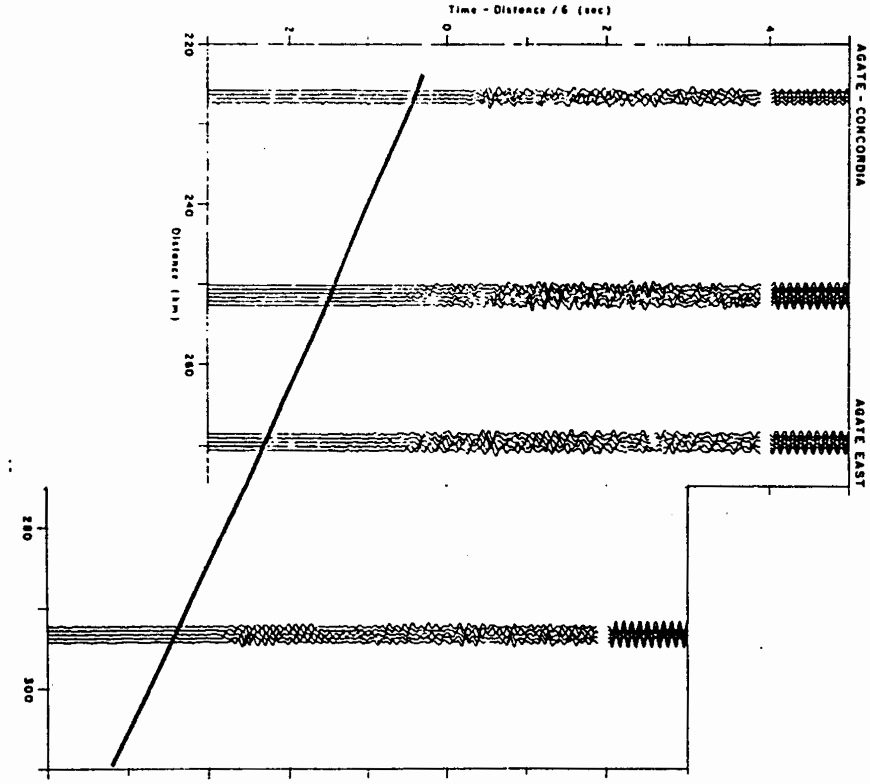
Time - Distance / 6 (sec)
AGATE - CONCORDIA
AGATE EAST
Distance (km)
220
240
260
280
300

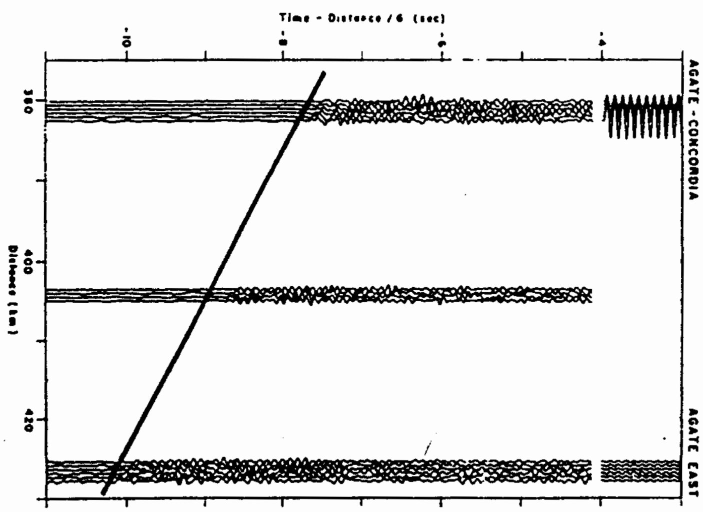
Time - Distance / 6 (sec)
-10
-8
-6
-4
AGATE - CONCORDIA
AGATE EAST
Distance (km)
380
400
420

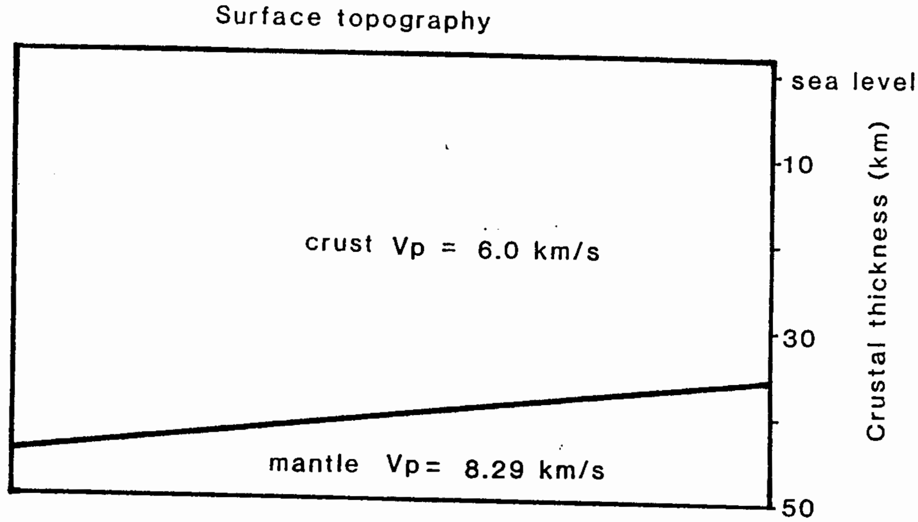

Figure B7.

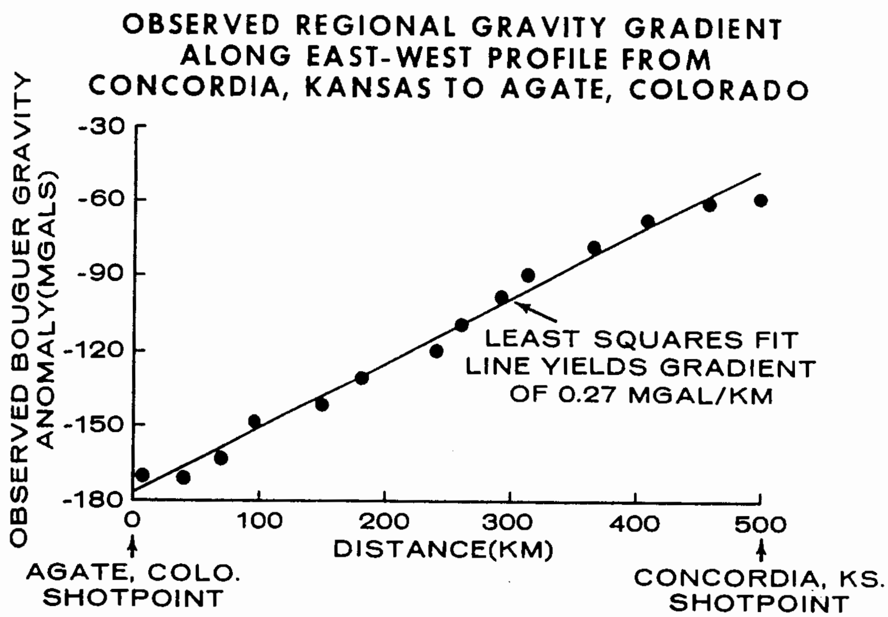

Figure B8.

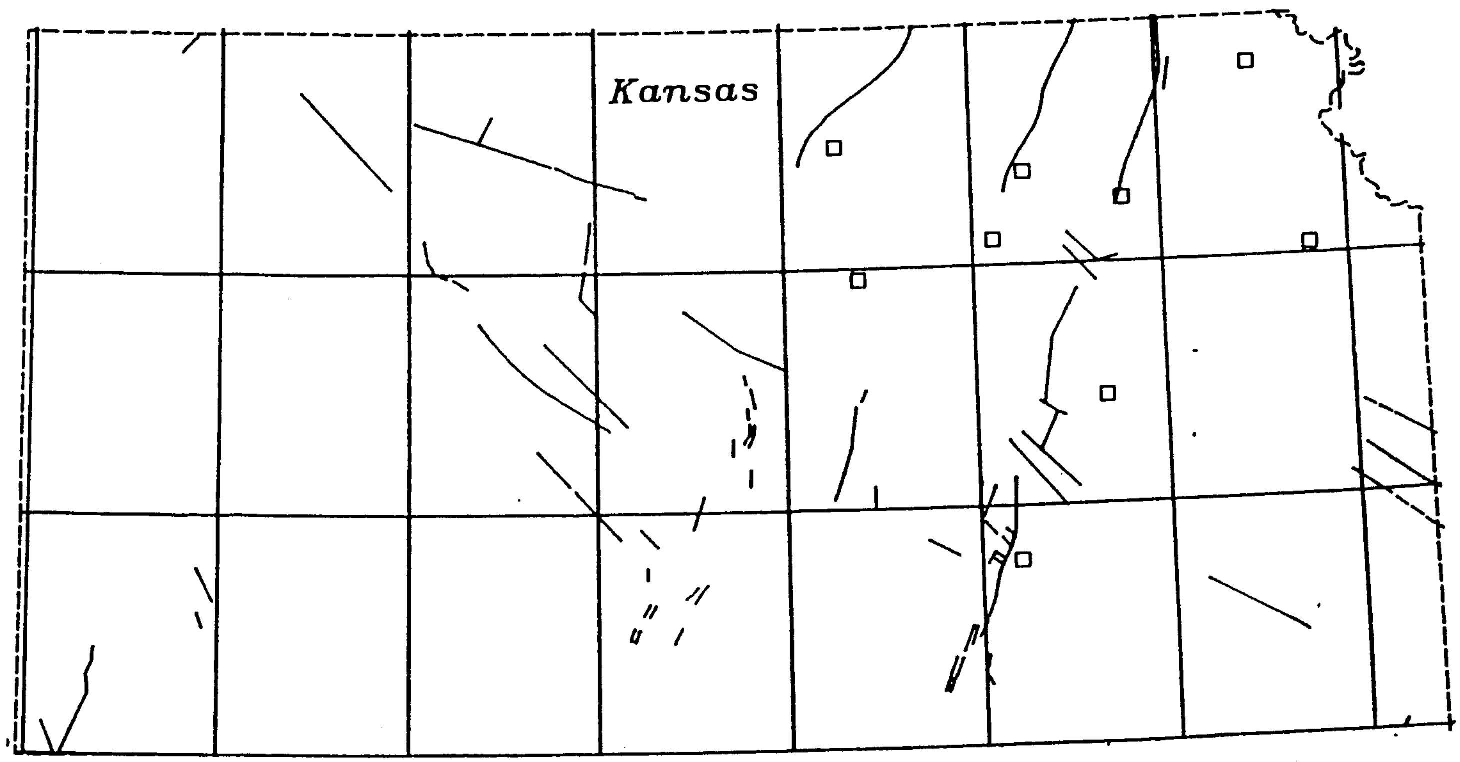

Figure B9.

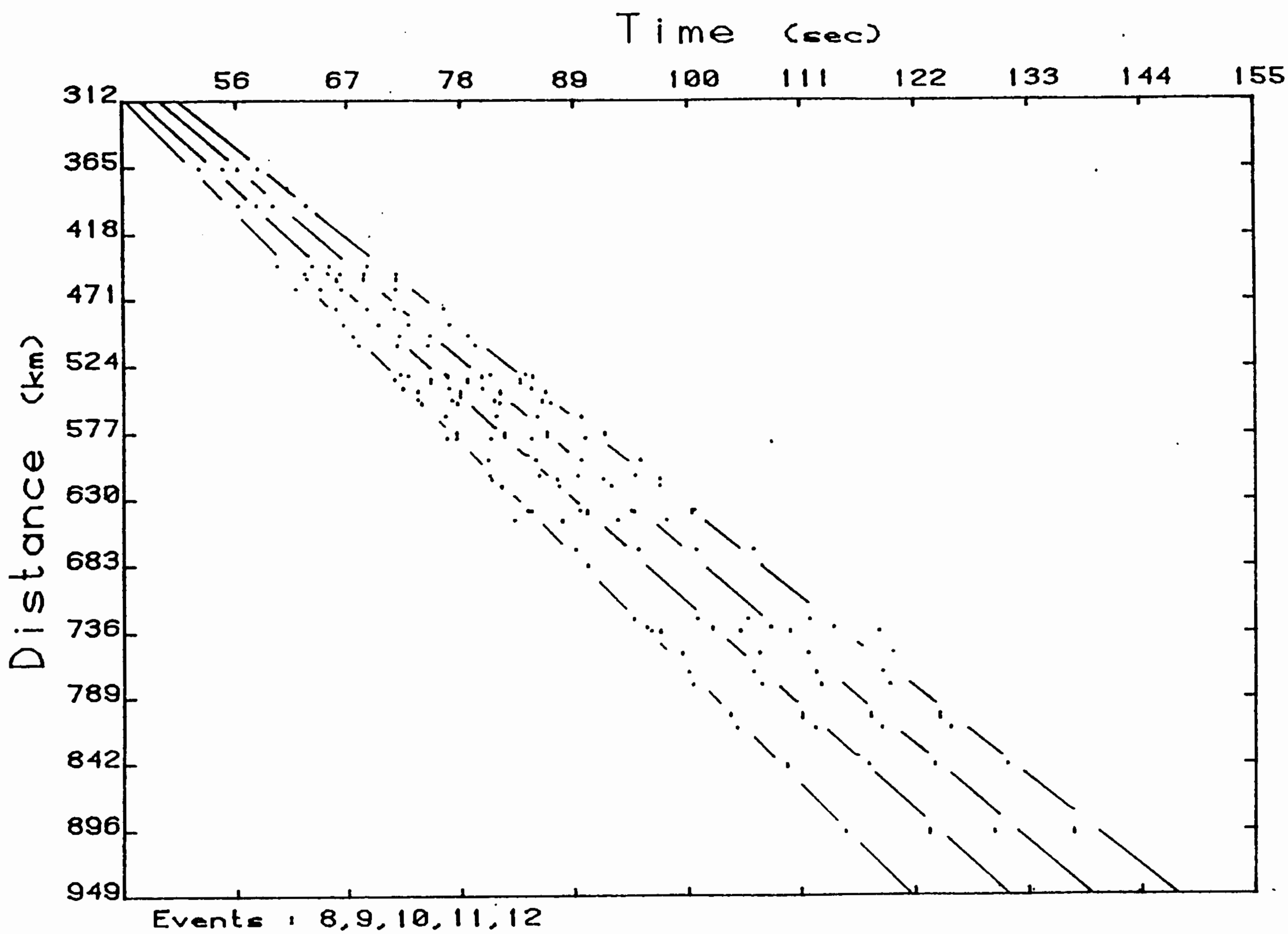

Time (sec)
56
67
78
89
100
111
122
133
144
155
Distance (km)
312
365
418
471
524
577
630
683
736
789
842
896
949
Events : 8,9,10,11,12

Figure B10.

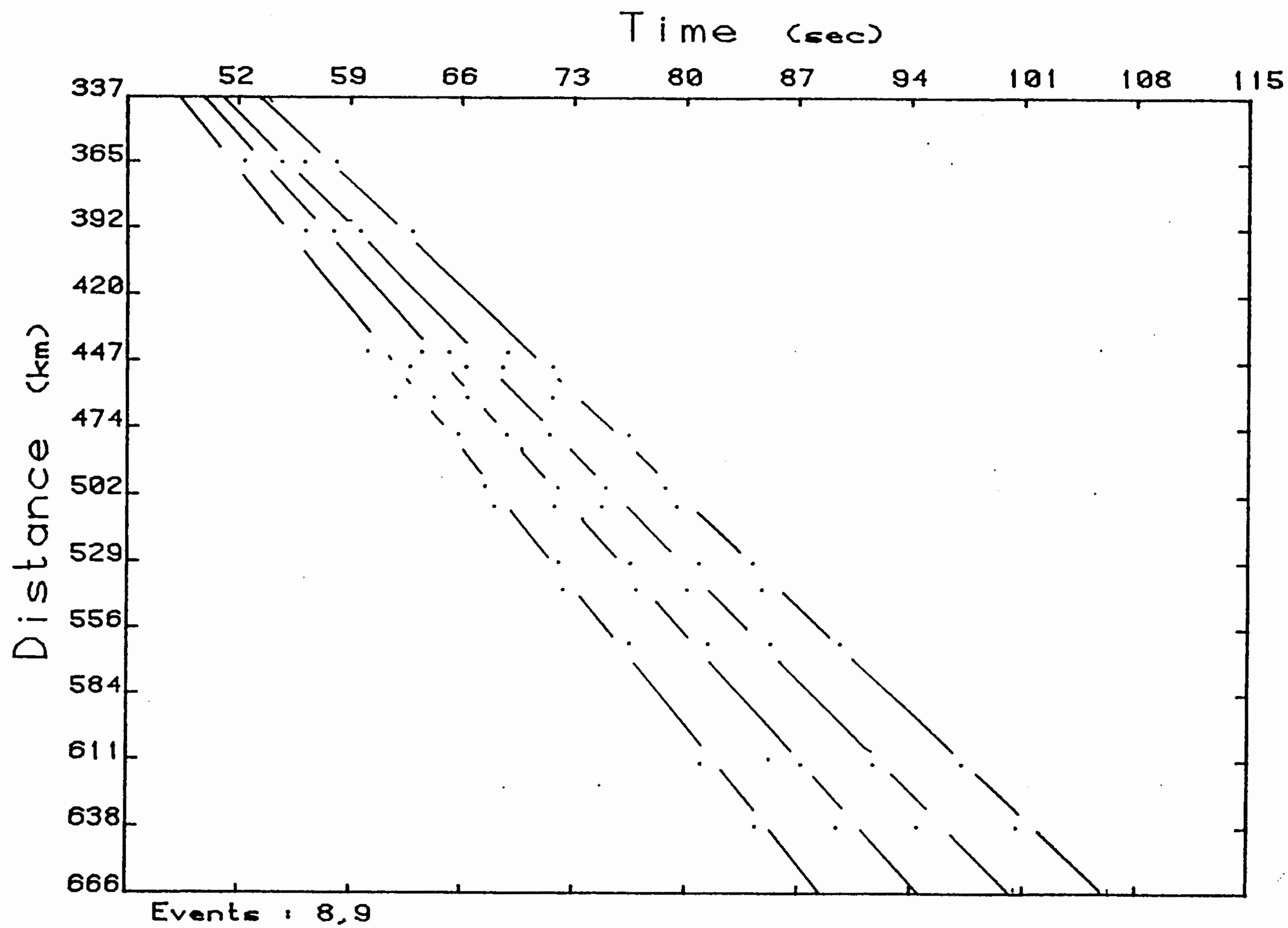

Time (sec)
52
59
66
73
80
87
94
101
108
115
Distance (km)
337
365
392
420
447
474
502
529
556
584
611
638
666
Events : 8,9

Figure B11.

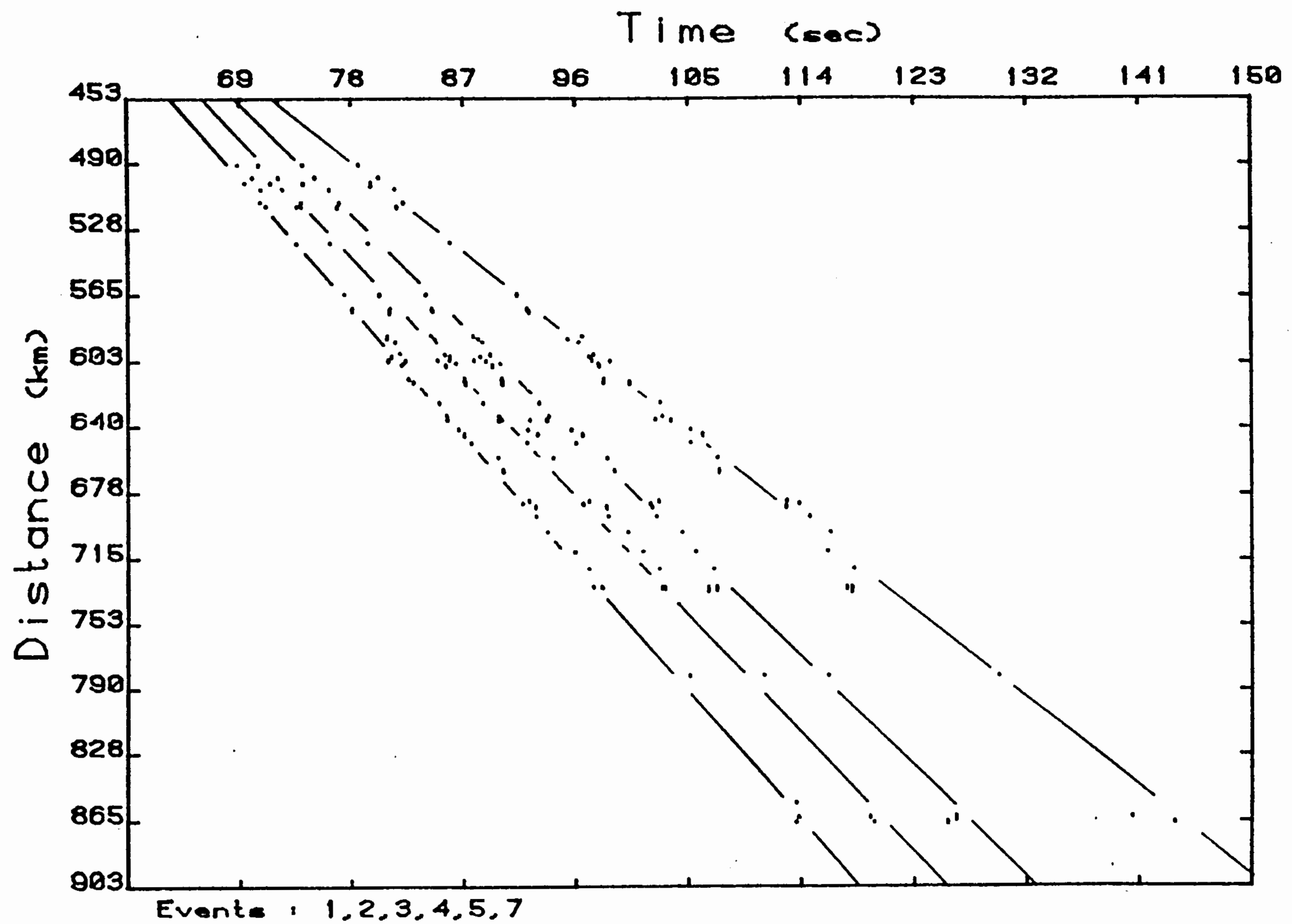
Time (sec)
69
78
87
96
105
114
123
132
141
150
Distance (km)
453
490
528
565
603
640
678
715
753
790
828
865
903
Events : 1,2,3,4,5,7

Figure B12.

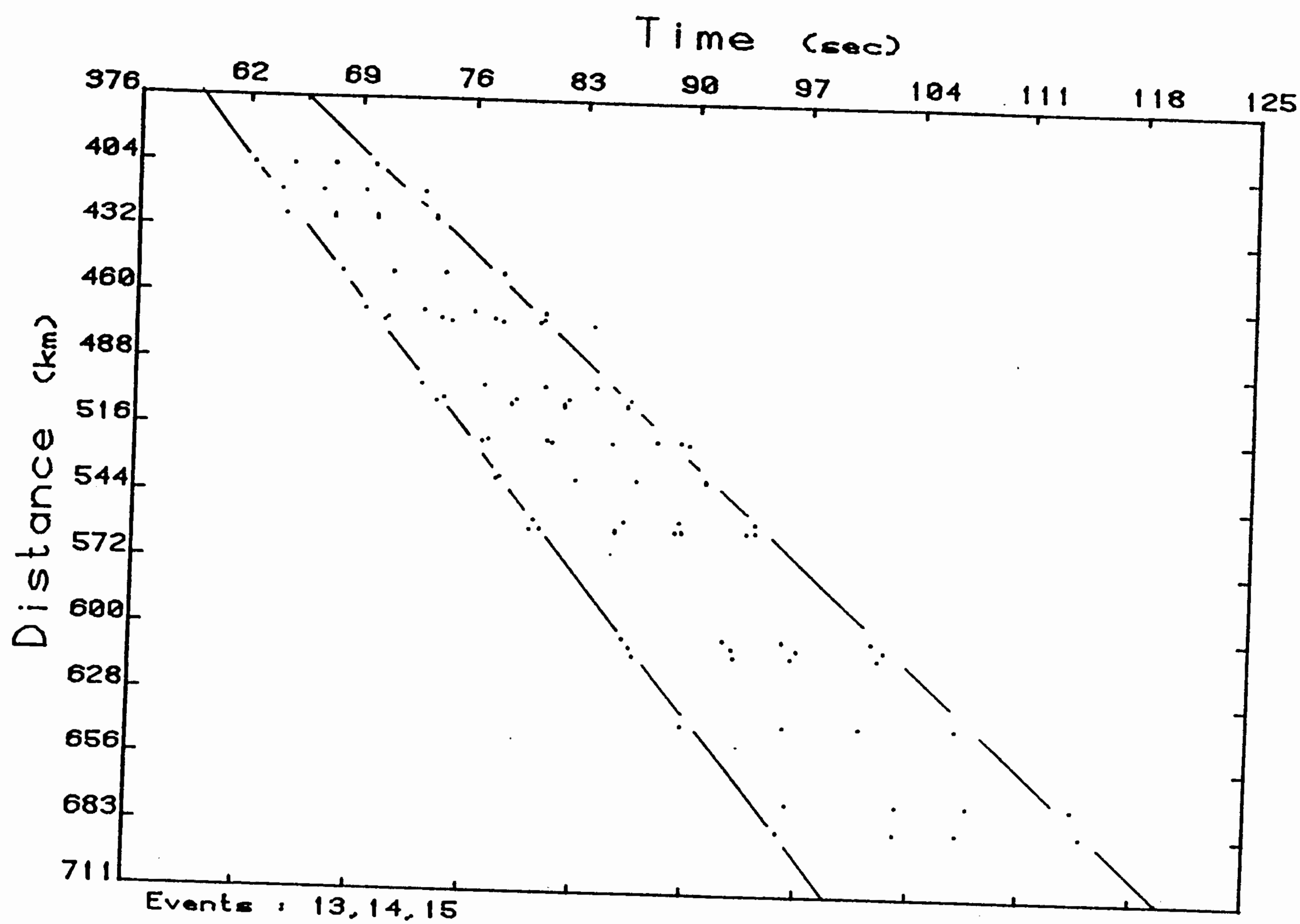
Time (sec)
62 69 76 83 90 97 104 111 118 125
Distance (km)
376 404 432 460 488 516 544 572 600 628 656 683 711
Events : 13,14,15

Figure B13.

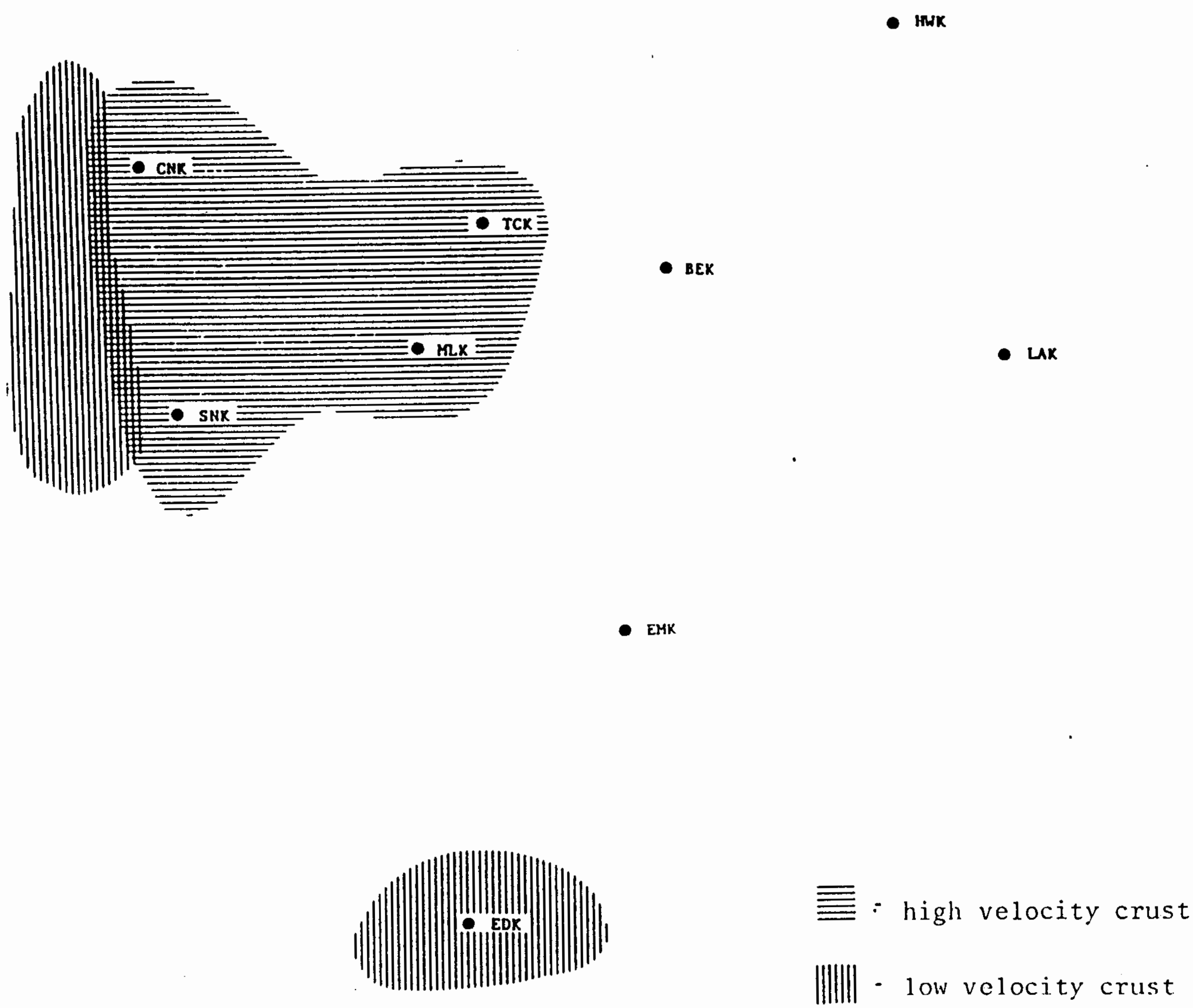
HWK
CNK
TCK
BEK
LAK
MLK
SNK
EMK
EDK
- high velocity crust
- low velocity crust

Figure B14.